International Council for the Exploration of the Sea (ICES)

ICES CM 2007/D:21
Theme Session D: ***Comparative Marine Ecosystem Structure and Function: Descriptors and Characteristics***

Fronts in the World Ocean's Large Marine Ecosystems

Igor M. Belkin and Peter C. Cornillon

Abstract. Oceanic fronts shape marine ecosystems; therefore front mapping and characterization is one of the most important aspects of physical oceanography. Here we report on the first effort to map and describe all major fronts in the World Ocean's Large Marine Ecosystems (LMEs). Apart from a geographical review, these fronts are classified according to their origin and physical mechanisms that maintain them. This first-ever zero-order pattern of the LME fronts is based on a unique global frontal data base assembled at the University of Rhode Island. Thermal fronts were automatically derived from 12 years (1985-1996) of twice-daily satellite 9-km resolution global AVHRR SST fields with the Cayula-Cornillon front detection algorithm. These frontal maps serve as guidance in using hydrographic data to explore subsurface thermohaline fronts, whose surface thermal signatures have been mapped from space. Our most recent study of chlorophyll fronts in the Northwest Atlantic from high-resolution 1-km data (Belkin and O'Reilly, 2007) revealed a close spatial association between chlorophyll fronts and SST fronts, suggesting causative links between these two types of fronts.

Keywords: Fronts; Large Marine Ecosystems; World Ocean; sea surface temperature.

Igor M. Belkin: Graduate School of Oceanography, University of Rhode Island, 215 South Ferry Road, Narragansett, Rhode Island 02882, USA [tel.: +1 401 874 6533, fax: +1 874 6728, email: ibelkin@gso.uri.edu].
Peter C. Cornillon: Graduate School of Oceanography, University of Rhode Island, 215 South Ferry Road, Narragansett, Rhode Island 02882, USA [tel.: +1 401 874 6283, fax: +1 874 6728, email: pcornillon@gso.uri.edu].

1. Introduction

Oceanic front is a relatively narrow zone of enhanced horizontal gradients of physical, chemical and biological properties (temperature, salinity, nutrients etc.) that separates broader areas of different vertical structure (stratification) (Fedorov, 1986; Belkin, 2003). Fronts occur on a variety of scales, from several hundred meters up to many thousand kilometers. Some of them are short-lived, but most are quasi-stationary and seasonally persistent: They emerge and disappear at the same locations during the same season, year after year. The most prominent fronts are present year-around. The temperature and salinity ranges (differences) across the strongest fronts could be as high as 10°- to 15°C and 2- to 3 parts per thousand (ppt), although somewhat smaller figures (5°C and 1 ppt) are much more common. The width of fronts vary widely; sometimes the frontal interface could be very narrow, less than 100 m, whilst some major fronts could be 50- to 200 kilometers wide. Vertically, many fronts extend several hundred meters in depth; major fronts extend as deep as 2000 meters. Fronts are crucial in various processes that evolve in the ocean and at the ocean interfaces with the atmosphere, sea ice and ocean bottom:

(1) Fronts are associated with current jets, so that any frontal pattern represents a circulation pattern;
(2) The along-frontal current jets are accountable for the bulk of water/heat/salt transport;
(3) Fronts separate different water masses and spawn rings responsible for the bulk of cross-frontal and meridional transport of water, heat and salt;
(4) Fronts usually coincide with major biogeographical boundaries associated with zones of enhanced bio-productivity, including fisheries grounds;
(5) The surface heat fluxes, wind stress and other meteorological parameters may differ drastically between the warm and cold sides of a front. Fronts strongly interact with the marine atmospheric boundary layer and separate regions with different response to atmospheric forcing, so they are crucial for weather forecasting and climate monitoring;
(6) Some high-latitude fronts are directly related to sea ice conditions, so the front locations are determined by the maximum extent of the sea ice cover;
(7) Fronts profoundly influence acoustic environment so that solving any sound propagation problem requires knowledge of the fronts' locations and characteristics;
(8) Ocean sedimentation regimes are largely determined by the circulation (hence frontal) pattern, therefore the interpretation of paleoceanographic and paleoclimatic information recorded in marine sediments requires a priori knowledge of the modern frontal situation;
(9) Because fronts are associated with convergent currents, oceanic and riverine pollutants can be concentrated thousands of times on fronts, thus endangering the fish, sea birds and marine mammals that inhabit the frontal zones.

Basic types of fronts. Fronts are formed by various processes; accordingly, there are several major frontal types, described below.

Estuarine fronts. These fronts form as interfaces between the freshwater river outflow (plume) and the ambient sea water. Consequently, they are mainly salinity fronts, although in most cases there is a temperature gradient as well across the principal salinity front. Since most rivers carry substantial amounts of sediments (silt), most estuarine fronts are turbidity fronts as well and therefore could be easily observed from space owing to the distinct color/transparency gradients across these fronts. Examples: Amazon River, Rio de la Plata, Chesapeake Bay, Yangtze River, and Ganges plume fronts.

Shelf fronts. These fronts are observed over the mid-shelf areas, well inshore of the shelfbreak. Their origin is sometimes related to the opposing currents over the shelf, with the offshore current typically flowing north (in the northern hemisphere) and the inshore current flowing south (e.g. the South Atlantic Bight). Example: Bering Sea, Middle Atlantic Bight and Eastern China Seas shelf fronts. Some shelf fronts are apparently related to the shelf's geomorphology, specifically, submerged terraces (paleo-shorelines), e.g. in the Bering Sea.

Tidal mixing fronts. In some shallow areas tides dissipate tremendous amount of energy through bottom friction. In such areas the water column might be completely mixed by the tides. Typically, the maximum depth where it happens is approximately 100 m, whereas the average depth is rather 50 meters. Consequently, a front forms between the completely mixed water column over the shallow depths and the stratified water column over the deeper bottom. Such fronts are observed over many shelves (e.g. in the North, Celtic, Bering, East China, Yellow, and Okhotsk Seas). The tidal mixing fronts also form around banks (e.g. Georges Bank), islands (e.g. Pribilof Islands in the Bering Sea) and peninsulas (e.g. Shandong Peninsula, Yellow Sea; Península Valdés, Patagonian Shelf).

Shelfbreak fronts. This is the most common frontal type; such fronts are aligned with the shelfbreak and separate the on-shelf water from the off-shelf (oceanic) water. The shelfbreak fronts are water mass fronts because they separate two distinct water masses, onshore and offshore (this is not the case, for example, with the tidal mixing fronts described above). There is always a well-defined current along the shelfbreak fronts. Examples: Mid-Atlantic Bight; Bay of Biscay.

Coastal upwelling fronts. Any upwelling (wind-induced, topographic or tidal) brings the subsurface water to the surface. Because the subsurface water is usually colder than the surface layer, a front emerges between the cold, upwelled water inshore and the warmer water offshore. Such fronts are observed off Washington-Oregon-California, Peru-Chile, northwest Africa, Angola-Namibia-South Africa, Yucatan Peninsula etc.

Equatorial upwelling fronts. The Coriolis force causes the equatorial divergence, with the surface waters moving away from the equator in both hemispheres. The colder subsurface water comes to the surface to create a temperature (and salinity) gradient at the contact with the warm surface water. Such fronts are prominent in the central and eastern Pacific and in the Atlantic Oceans. The land mass asymmetry of the Indian Ocean boundaries might be the main reason why the equatorial upwelling fronts are not prominent in the Indian Ocean.

Western boundary current fronts. Fronts associated with the Gulf Stream, Kuroshio, Agulhas Current, Brazil, and East Australia Currents are the world's strongest in terms of the cross-frontal ranges of oceanographic properties, vertical extent, along-front current speed and transport, and other characteristics. These fronts could be traced into the open ocean for many thousand kilometers. In winter, two fronts are distinct on both sides of the western boundary currents because each current carries the tropical water which is warmer then the ambient waters inshore and offshore of the currents.

Subtropical convergence fronts. These fronts form because of the Ekman wind convergence that brings together waters of different temperature (because of the north-south large-scale temperature gradient in the ocean) and maintains the emerging front. Such fronts are observed in the North Atlantic (Sargasso Sea) and North Pacific, and in the southern parts of the Atlantic, Indian, and Pacific Oceans.

Marginal ice zone fronts. These fronts are associated with the sea ice edge and very specific processes that operate within this zone. During sea ice formation, the brine rejection (salt release) causes haline convection. During the sea ice melt, the surface freshening creates a local salinity front between the low-salinity melt water and the ambient water. In spring, as the melt water absorbs solar radiation, a temperature gradient (thermal front) develops across the initial salinity front. Examples: Labrador, Greenland, Barents, and Bering Seas, and the Southern Ocean.

Southern Ocean fronts. This is the only ocean with truly circumpolar fronts, the Subantarctic, Polar, and Southern Antarctic Circumpolar Current fronts, whereas the Southern Subtropical Front is nearly-circumpolar. The origin of the above fronts is related to the dynamics of the Antarctic Circumpolar Current. The Antarctic Slope Front forms between the shelf water near the Antarctic continent and the offshore oceanic water, therefore it could be considered as one of the shelfbreak fronts. However, its structure and dynamics are different from other shelfbreak fronts. Katabatic winds from the Antarctic continent help maintain the westward current over the Antarctic shelf, thus playing a role in the Antarctic slope front maintenance.

Societal importance and applications. Fronts are important in the following applications:
Marine transportation: Frontal locations and their characteristics are used to optimize ship routing depending on area and season and the observed long-term (interannual and decadal) variability of ocean fronts and associated currents;
Fishing industry: Many important fishery grounds, including some underexploited fish stocks, are located along fronts;
Climate change monitoring and prediction requires adaptive strategy for the global ocean observing system, based on all available information about the location and variability of major ocean currents (i.e. fronts) to optimize construction, deployment and utilization of observational platforms;
Marine mining, including oil and gas industry, uses information on the pattern and persistence of ocean currents (hence fronts and frontal eddies, including rings) that directly affect drilling operations and production cycle on offshore platforms;
Pollution control, waste disposal and hazards mitigation benefits from the knowledge of current (i.e. frontal) pattern and its variability, especially in the regions influenced by strong frontal currents and rings (e.g. the U.S. East Coast and the Gulf of Mexico);
Integrated coastal zone management is dependent on the exact knowledge of potential vulnerability of the managed areas to nature hazards (hurricanes, storms, floods, tornados) which frequency and spatial pattern are dependent on the large-scale ocean circulation/frontal system;
Submarine navigation is facilitated by incorporation into computer acoustic and circulation models of detailed information on the locations and characteristics of fronts.

2. Data and Method

The approach used in this study is based on ***histogram analysis***. Since a front is a boundary between two relatively uniform water masses, histograms of any oceanographic characteristic (e.g. SST) in the vicinity of the front should have two well-defined modes that correspond to the water masses divided by the front, while the latter corresponds to the frequency minimum between the modes. This basic idea has been implemented by Cayula et al. (1991), Cayula and Cornillon (1992, 1995, 1996) and Ullman and Cornillon (1999, 2000, 2001); the reader is referred to these works for all the pertinent details. The fronts used for this study were derived from the NOAA/NASA Pathfinder SST fields (Vazquez et al., 1998) for the period 1985-1996, covering almost entire World Ocean, from 75°N to 75°S. These fields were obtained from the AVHRR Global Area Coverage data stream (two 9.28-km resolution fields per day) and are available from the Jet Propulsion Laboratory. SST fronts were obtained from the cloud-masked SST fields with the multi-image edge detection algorithm (Cayula and Cornillon, 1996; Ullman and Cornillon, 1999, 2000, 2001). The cloud masking and front detection algorithms were applied to each of the 8,364 SST images in the 12-year sequence. The frontal data were aggregated over months (e.g. 12 Januaries taken together), and seasons (e.g., the winter climatology is obtained from all Januaries, Februaries, and Marches taken together). The front detection and tracking is conducted at three levels: window, image and a sequence of overlapping images. The optimum window size is important. Based on a series of numerical experiments with various window sizes, Cayula and Cornillon (1992) have arrived at the optimum window size of 32 by 32 pixels. The front detection algorithm uses all pixel-based SST values within each window to compute a SST histogram for the given window. For each window that contains a front (a relatively narrow zone of enhanced SST gradient), the corresponding SST histogram would have a frequency minimum identified with the front. Three basic types of maps are used in the analysis: *long-term frontal <u>frequency maps</u>*, *quasi-synoptic frontal <u>composite maps</u>*, and *long-term frontal <u>gradient maps</u>*. The long-term frontal *<u>frequency maps</u>* show the pixel-based frequency F of fronts normalized on cloudiness: For each pixel, F = N/C, where N is the number of times the given pixel contained a front, and C is the number of times the pixel was cloud-free. Thus, the frequency maps are best suited for displaying most stable fronts. At the same time, frontal frequency maps understate some fronts associated with widely meandering currents such as the Gulf Stream Extension, North Atlantic Current, and Azores Current. In such cases quasi-synoptic frontal *<u>composite maps</u>* are most helpful because they present all of the synoptic snapshots of the "instant" fronts detected in individual SST images within a given time period (e.g. week, month, or season), without any averaging or smoothing. The frontal composite maps thus allow one to detect the most unstable fronts that are not conspicuous in the frontal frequency maps. The *long-term frontal <u>gradient maps</u>* show two scalar quantities, *<u>gradient magnitude</u>* and *<u>gradient direction</u>*, associated with each frontal pixel in the long-term frontal frequency maps. Gradient visualization by color mapping gradient magnitude and direction (e.g. Ullman and Cornillon, 1999) has a clear advantage over vector mapping, namely resolution. Scalar mapping allows even tiny details to be preserved, down to a single pixel, whereas vector mapping typically requires sub-sampling, otherwise vector maps become crowded and illegible.

3. Results: Frontal Patterns in Individual Large Marine Ecosystems

Frontal schematics for all 64 World Ocean's Large Marine Ecosystems (**<u>Figure 1</u>**; **<u>Plates 1-4</u>**) were derived from the 12-year (1985-1996) data bank of frontal maps generated automatically with the Cayula-Cornillon front detection algorithm from 9-km Pathfinder SST data and assembled at the University of Rhode Island (Belkin, 2005). These frontal schematics are long-term annual means. Only the most robust fronts in each LME are shown. We have chosen to show all well-defined fronts regardless of the seasons during which they develop and peak, so at any given time, typically, only some fronts can be observed, but not all of them at once, in each LME. The frontal paths shown in these maps portray long-term mean frontal patterns; these patterns are briefly discussed below. Seasonal and interannual variability of fronts in each LME will be covered in separate publications elsewhere.

<u>LME #01: Eastern Bering Sea</u>

Five major fronts are distinguished over the Eastern Bering Shelf and Slope (Belkin and Cornillon, 2005). The Coastal Front consists of three segments, the Bristol Bay Front (BBF), the Kuskokwim Bay Front (KBF), and Shpanberg Strait Front (SSF), all of them extending approximately parallel to the Alaskan Coast over 10-to-20-m depth. Farther offshore, the Inner Shelf Front (ISF) is located over 20-to-40-m depth while the Mid-Shelf Front (MSF) is found over 40-to-60-m depth. These two fronts are also approximately isobathic. The most distant offshore fronts, Outer Shelf Front (OSF; 60-100-m depth) and the Shelf-Slope Front (SSF; 100-200-m depth within this LME) are not isobathic. They extend from relatively shallow depths in the east, off Bristol Bay, to significantly larger depths in the west, where the SSF crosses the shelf break and slope to continue over the deep basin as it leaves LME #01 and enters LME #53.

LME #02: Gulf of Alaska

The Polar Front (PF) exists year-round in the western part of the Gulf (Belkin et al., 2002). This front is associated with the Subarctic Current that crosses the North Pacific from Hokkaido to the Gulf of Alaska where it retroflects and flows along the Aleutian Island Chain, branching first into the Eastern Bering Sea (LME #01), then into the Western Bering Sea (LME #53). Several fronts develop in summer over the Alaskan Shelf (Belkin and Cornillon, 2003; Belkin et al., 2003). The most conspicuous Kodiak Front (KF) is observed east and south of Kodiak Island, where its quasi-stable location is controlled by local topography. The Inner Passage Front (IPF) is located in a strait between the Queen Charlotte Islands and the British Columbia coast (Belkin and Cornillon, 2003; Belkin et al., 2003).

LME #03: California Current

The California Current Front (CCF) separates relatively cold, low-salinity waters of the southward California Current from warmer and saltier waters inshore (Hickey, 1998). The Subarctic Front (SAF) separates the northward Subarctic Current from inshore waters. On the inshore side of the California Current, upwelling fronts develop in summer (Belkin and Cornillon, 2003; Belkin et al., 2003). Offshore frontal filaments, sometimes hundred kilometers long, carry the upwelled cold, nutrient-rich water across the entire LME (Belkin and Cornillon, 2003). In winter, the poleward Davidson Current develops over the shelf and slope, giving rise to a seasonal front (DCF) between warm saline subtropical waters inshore and colder, fresher temperate waters offshore. The Davidson Current Front can be traced from off southern California (35°N) northward up to the northern Washington coast (48-49°N).

LME #04: Gulf of California

This is the smallest LME landlocked between Baja California and Mexico’s mainland. Temperature contrast between the northern and southern Gulf is 2 to 3°C, depending on the season. This gradient is enhanced along a bathymetric step in the middle of the Gulf, where a thermal front is observed (Inner Gulf Front, IGF). Other fronts form between Mexico’s mainland and Baja California where Pacific inflow waters meet resident waters of the Gulf of California (Outer Gulf fronts, OGF; Belkin et al., 2007). The Pacific and resident waters have different salinities (in addition to different temperatures); the salinity differential is the main factor responsible for the maintenance of this front.

LME #05: Gulf of Mexico

Two major fronts emerge in winter from December through March, over two shelf areas, the West Florida Shelf (WFS) and Louisiana-Texas Shelf (LTS) (Belkin et al., 2007). The WFS Front (WFSF) extends over the mid-shelf, whereas the LTS Front (LTSF) is located closer to the shelf break. Both fronts form owing to cold air outbreaks (e.g. Huh et al., 1978). Huge freshwater discharge from the Mississippi River Estuary (MRE) and rivers of the Florida Panhandle contributes to the fronts’ development and maintenance. Compared to these northern fronts, the Campeche Bank Shelf-Slope Front (CBSSF) and Campeche Bank Coastal Front (CBCF) in the south are weak and unstable (Belkin et al., 2007). The Loop Current Front (LCF) is always present at the inshore boundary of the namesake front, best defined in winter.

LME #06: Southeast U.S. Continental Shelf

This LME coincides with the South Atlantic Bight. Here the northward warm, saline Gulf Stream is bounded by two fronts. The inshore Gulf Stream Front (IGSF) extends over the upper continental slope and shelf break (approximately aligned with the 50-m isobath; Atkinson and Menzel, 1985), while the offshore Gulf Stream Front (OGSF) runs parallel to the IGSF, approximately 100 km offshore of the latter. This LME is radically different from LME #07 (Northeast U.S. Shelf) that occupies the Mid-Atlantic Bight where the Shelf-Slope/Shelf Break Front is associated with a cold, fresh southward Slope Current. The Gulf Stream forms a semi-permanent offshore deflection near a deepwater bank SE of Charleston, NC, called the "Charleston Bump" (CB), at 31.5°N. The Mid-Shelf Front (MSF) is aligned approximately with the 35-to-40-m isobaths. Other shelf fronts separate a mélange of water masses formed by wintertime cold air outbreaks, river discharge, tidal mixing and wind-induced coastal upwelling (Pietrafesa et al., 1985; Belkin et al., 2007).

LME #07: Northeast U.S. Continental Shelf

This LME includes the Mid-Atlantic Bight and Gulf of Maine. The Shelf-Slope Front (SSF) forms the offshore boundary of this LME associated with a southward flow of cold, fresh water that originates in the Labrador Current. This flow/front retroflects as it approaches Cape Hatteras to merge with the Gulf Stream. The Mid-Shelf Front (MSF) extends over the 50-m isobath along the entire Mid-Atlantic Bight (Ullman and Cornillon, 1999; Belkin et al., 2007). The Nantucket Shoals Front (NSF) is the shallowest in this LME; it squirts the namesake bank/shoals and roughly coincides with 20-to-30-m isobaths. The Gulf of Maine fronts separate deep basins (Wilkinson and Jordan) from major banks (Georges and Browns); these fronts are best defined in winter (Belkin et al., 2007). Georges Bank is surrounded by a tidal mixing front, GBF (Mavor and Bisagni, 2001). The Main Coastal Front (MCF) develops seasonally off Maine (Ullman and Cornillon, 1999). The Cape Cod Front (CCF) emerges seasonally between Cape Cod and Georges Bank. The above SST fronts are collocated with chlorophyll fronts (Belkin and O'Reilly, 2007).

LME #08: Scotian Shelf

The Shelf-Slope Front (SSF) along the Scotian Shelf/Slope bounds this LME and is associated with the southward cold, fresh Labrador Current, augmented by fresh discharge from the Gulf of St. Lawrence. The Gulf component is strongly seasonal that reflects in the SSF characteristics (Linder and Gawarkiewicz, 1998). The newly-identified Gully Front (GF) is observed at 43.5°N over the Gully, the largest canyon that incises the Scotian Shelf and Slope. Medium-scale thermohaline fronts in the southern Gulf of St. Lawrence are generated seasonally by spring freshet, followed by summertime warming. The Cabot Strait Front (CSF) is also related to the Gulf of St. Lawrence fresh outflow (Belkin et al., 2007). The Cape North Front (CNF) develops north of the Cape Breton Island.

LME #09: Newfoundland-Labrador Shelf

The Labrador Shelf-Slope Front (LSSF) extends along the shelf break and upper slope. The Labrador Mid-Shelf Front (LMSF) recently identified from satellite data runs inshore of the LSSF, parallel to Labrador. Farther downstream, the LMSF hugs Newfoundland and merges with the LSSF south of Newfoundland, near 45°N and 55°W (Belkin et al., 2007). The Flemish Cap, a shallow bank that supports important fisheries, is surrounded by the Flemish Cap Front

(FCF) that isolates on-bank waters from direct contact with off-bank oceanic waters. The FCF can be considered an offshore branch of the LSSF. The main branch of the LSSF continues south via Flemish Pass between the Grand Banks of Newfoundland and Flemish Cap.

LME #10: Insular Pacific-Hawaiian

This is the only LME located in the middle of an ocean. Meteorological and oceanographic conditions within this LME are relatively uniform on the Pacific Ocean scale; they can be characterized as subtropical. This relative uniformity is interrupted by the Subtropical Front (STF) that cuts across this LME at 25°-26°N in winter and 28°-29°N in summer. This seasonal shift of the STF is caused by a corresponding meridional shift of the wind field convergence, which is ultimately responsible for the STF formation. The STF sometimes consists of two nearly parallel fronts a few degrees of latitude apart that form the double Subtropical Frontal Zone, similar to the double frontal zones found in other subtropical oceans (Belkin et al., 2007). The STF plays an important role in ocean ecology as it defines a major trans-ocean migration path and feeding ground of various fish species, including apex predators such as tuna, and also turtles, e.g. loggerheads.

LME #11: Pacific Central-American Coastal

Most fronts within this LME are generated by coastal upwelling. Some fronts off the Pacific coast of Central America originate owing to quasi-regular bursts of topographically generated winds blowing from the Caribbean across Central America toward the Pacific Ocean. Local orography tends to channel these winds and make their direction exceptionally stable and predictable, especially in the Gulf of Tehuantepec where these winds result in formation of upwelling zones and fronts that bound them extending far offshore (Belkin and Cornillon, 2003). This is the only place in the World Ocean where such fronts are observed.

LME #12: Caribbean Sea

In the southern Caribbean Sea fronts are generated by coastal wind-induced upwelling off Venezuela and Colombia at 75°-78°W, 70°-75°W, and 62°-66°W (Belkin et al., 2007). A 100-km-long front dissects the Gulf of Venezuela along 70°40'W, likely caused by the brackish outflow from Lake Maracaibo combined with coastal upwelling. Two shelf-break fronts off Cuba encompass two relatively wide shelf areas off southern Cuban coast, east of Isla de la Juventad (83°W) and along the Jardines de la Reina island chain (79°-80°W), both best developed in winter. The Windward Passage Front between Cuba and Hispaniola (73°W) separates the westward Atlantic inflow waters moving into the Caribbean in the western part of the passage from the Caribbean outflow waters heading eastward in the eastern part of the passage. A 200-km-long front in the Gulf of Honduras peaks in winter, likely related to a salinity differential between the Gulf's apex and offshore waters caused by high precipitation in southern Belize (Heyman and Kjerfve, 1999).

LME #13: Humboldt Current

The most important front off Peru is caused by wind-induced coastal upwelling. The Peruvian Upwelling Front (PUF) extends along the shelf break from 5°S to 19°S. Farther south, the coastline sharply changes its orientation and is no longer favorable to wind upwelling. A new summertime front has been described from satellite data, called the Nazca Front (NF) because of its proximity to the Nazca Ridge (Belkin and Cornillon, 2003). The Nazca Front (NF) departs from Chilean coast at 25°S-27°S and extends northwestward, best developed in March. This front is a major tuna fishing ground, especially important for yellowfin tuna fishery. The Subtropical Frontal Zone, bounded by the North and South Subtropical Fronts (NSTF and SSTF respectively), crosses the South Pacific zonally between 35°S-40°S, impinges Chilean coast and bifurcates, with its branches flowing meridionally but in the opposite directions along Chilean coast. The attendant fronts between the Subtropical Frontal Zone waters and Chilean coastal waters are observed year-round. South of 40°S, the Chiloe Archipelago low-salinity waters form a salinity front at the contact with oceanic waters.

LME #14: Patagonian Shelf

Three year-round fronts are distinguished over the Patagonian Shelf: Valdes Front (VF) at 42°S, San Jorge Front (SJF) at 46°S and Bahia Grande Front (BGF) at 51°S. The origin of VF and SJF might be related to intense tidal mixing (Glorioso, 1987; Glorioso and Flather, 1995, 1997). Two seasonal fronts are the Bahia Blanca Front (BBF) at 39°S and Magellan Front (MF), the latter consisting in fall (April-June) of two branches, the Patagonian-Magellan Front (PMF) and Tierra del Fuego Front (TFF). The origin of MF and its branches is related to the influx of cold, fresh Pacific water via the Strait of Magellan (Belkin et al., 2007). The offshore boundary of this LME coincides with the Falkland (Malvinas) Front/current that extends along the Patagonian shelf break and upper continental slope of the Argentinean Sea.

LME #15: South Brazil Shelf

The Brazil Current Front forms the offshore boundary of this LME. This current transports equatorial waters from off Cabo de São Roque (5°30'S) down to 25°S, where the thermal contrast with colder shelf waters is enhanced in winter-spring by an equatorward flow of cold, fresh Argentinean shelf water reaching as far north as 23°S (Campos et al., 1995, 1999; Ciotti et al., 1995; Lima et al., 1995, 1996). Shelf-slope fronts (SSF) in the South Brazil Bight and off Rio Grande do Sul are year-round, best defined from April through September (Belkin et al., 2007). The Subtropical Shelf Front off southern Brazil has been recently described by Piola et al. (2000) and Belkin et al. (2005).

LME #16: East Brazil Shelf

This LME includes the bifurcation of the westward South Equatorial Current near Cabo de São Roque (5.5°S; Belkin et al., 2007) that gives rise to two currents and associated fronts: the northward North Brazil Current Front (NBCF) and the southward South Brazil Current Front (SBCF). Within this LME the southward SBCF is most noticeable in salinity; it becomes distinct as a temperature front from the South Brazil Bight southward (see LME #15). The northward NBCF is year-round, best defined in austral winter; it extends along the coast into LME #17. The Southern Bahia Front (15°S-19°S) and the Cabo Frio Front (20°S-24°S) are caused by wind-induced upwelling and are best developed during austral summer and fall, from January through June (Belkin et al., 2007).

LME #17: North Brazil Shelf

Major fronts within this LME are associated with the Amazon River outflow and, to a lesser extent, the Orinoco River outflow. The Amazon plume initially turns northwestward and flows along the Brazil coast as the North Brazil Current. Off the Guiana Coast, between 5°N and 7°N, the North Brazil Current retroflects and flows eastward. This retroflection develops seasonally

(Belkin et al., 2007) and produces anticyclonic (clockwise-rotating) rings of warm, low-salinity water that propagate northwestward toward the Barbados, Lesser Antilles Islands and eventually the Caribbean Sea. The second major source of fresh water is the Orinoco River plume. Most thermal fronts are associated with salinity fronts related to fresh lenses and plumes originated at the Amazon and Orinoco estuaries. Such fronts are relatively shallow, sometimes just a few meters deep. Nonetheless, these fronts are important to many species whose ecology is related to the upper mixed layer. Fresh lenses generated by the Amazon and Orinoco outflows persists for months, largely owing to the sharp density contrasts across TS-fronts that form their boundaries (in case of fresh, warm tropical lenses, the temperature and salinity contributions to the density differential reinforce each other).

LME #18: West Greenland Shelf

The West Greenland Current Front (WGCF) closely follows the shelf break and the steep upper slope until 52°W, where the slope becomes notably less steep and therefore no longer stabilizes the WGCF (Belkin et al., 2007). The front instability results in eddy generation that enhances cross-frontal exchange of heat, salt and nutrients as well as larvae and juvenile fish. The WGCF waters originate partly in the cold, fresh East Greenland Current and partly in the warm and salty Irminger Current. The Mid-Shelf Front (MSF) runs over mid-shelf roughly parallel to the coast and carries very cold, low-salinity polar water originated in the East Greenland Current augmented by melt water from the Greenland Ice Sheet.

LME #19: East Greenland Shelf

The East Greenland Polar Front (EGPF) hugs the shelf break and the Greenland continental slope and serves as the offshore boundary of this LME (Belkin et al., 2007). The EGPF waters originate in the Arctic Ocean that explains their extremely low temperature and salinity. The EGPF forms a complicated pattern over the broad Ammassalik Shelf, between 63°N-65°N, where three separate branches of the EGPF are observed (Belkin et al., 2007). This shelf is known as a major spawning area of cod, therefore the multiple frontal structure discovered from satellite data is important to the local cod fishery. South of the Denmark Strait, the EGPF is joined by the Irminger Current Front that carries warm and salty waters originated in the North Atlantic Current.

LME #20: Barents Sea

The Atlantic flow enters the Barents Sea along the Norwegian coast and continues along Russia's coast, carrying warm and salty waters that form distinct TS-fronts at the contact with coastal waters and resident waters of the Barents Sea proper (Belkin et al., 2007). North of Tromse and Nordkapp two fronts are distinguished, a coastal front just few miles off of the coast and an offshore front farther out to sea. The Polar Front (PF) south of Bear Island follows the Spitsbergen (Svalbard) continental slope that provides bathymetric steering to the front and ensures its stability. In the absence of topographic steering elsewhere within the Barents Sea, the Polar Front's location is variable and depends largely on the intensity of the Atlantic inflow to the Barents Sea.

LME #21: Norwegian Sea

The North Atlantic Current Front (NACF) exists year-round between warm and salty Atlantic waters transported by the current into the Norwegian Sea, and resident waters of the Norwegian

Sea (Belkin et al., 2007; Kostianoy et al., 2005). The Norwegian Coastal Current Front (NCCF) hugs Norway's coast; this current carries northward low-salinity waters from the North Sea with an admixture of the Baltic Sea waters. The Arctic Front (AF) follows the Mid-Atlantic Ridge meridionally up to Jan Mayen, then turns NE along Mohns Ridge, then turns NNW along Knipovich Trough. The Iceland-Faroes Front (IFF) runs near this LME's southern boundary, spawning warm and cold eddies responsible for the bulk of cross-frontal exchange of heat, salt and nutrients. Decadal-scale "Great Salinity Anomalies" traveled across this LME in the 1970s, 1980s and 1990s (Belkin et al., 1998; Belkin, 2004).

LME #22: North Sea

Up to ten fronts have been distinguished in the North Sea from satellite data (Belkin et al., 2007). The North Atlantic Current enters the North Sea from the North; its branches are associated with the Fair Isle Front (FIF) and Shetland Front (ShF). The Norwegian Coastal Current Front (NCCF) extends along the Norwegian Coast and separates the low-salinity near-shore waters from Atlantic waters. Tidal mixing fronts form around Dogger Bank (DBF) and off Flamborough Head (FHF). The Atlantic waters entering the North Sea via the English Channel form two fronts, western (WECF) and eastern (EECF) at their contact with resident waters; these fronts flank the Atlantic inflow. The Frisian Front (FF) origin is related to the fresh outflow from the Rhein River and Shelda River. The Skagerrak Front (SkF) is located at the boundary with the Baltic Sea waters.

LME #23: Baltic Sea

Several fronts exist within the Baltic Sea (Belkin et al., 2007), namely the Bothnian Bay Front (BBF), Bothnian Sea Front (BSF), North Baltic Proper Front (NBPF), South Baltic Proper Front (SBPF), Gotland Front (GF), Irbe Strait Front (ISF), and Arkona Front (AF). Most fronts are topographically controlled: BBF and BSF encircle the respective depressions, while NBPF, SBPF, and GF extend along 100-m isobath that outlines the Baltic Proper basin. The ISF is situated over the outer edge of a sill that separates the Gulf of Riga from the Baltic Proper. Some fronts are distinct year-round, namely BSF, NBPF and SBPF. Other fronts emerge and persist seasonally.

LME #24: Celtic-Biscay Shelf

The most important front within this LME is the Shelf-Slope Front (SSF) that extends along the shelf break/upper continental slope from the Bay of Biscay around the British Isles up to the Faroe-Shetland Channel where it joins the North Atlantic Current Front (Belkin et al., 2007). This front is distinct year-round, best defined in fall when its separation from the Mid-Shelf Front (MSF) becomes evident. The SSF is associated with the Shelf Edge Current, believed to be continuous all the way up to the Faroe-Shetland Channel. The SSF, however, does not appear continuous suggesting that the Shelf Edge Current is likely not continuous all the time. The areas where the SSF is broken most often are near Goban Spur and Porcupine Bank; these bathymetric features are clearly responsible for the front's instabilities in these areas. The Mid-Shelf Front (MSF) is located between the SSF and the coasts of France, United Kingdom and Ireland. Tidal mixing fronts exist off Ushant Island, south of the Irish Sea, south of Ireland, and over the Malin Shelf.

LME #25: Iberian Coastal

Frontal pattern off Iberia is fairly complicated and variable, especially on the seasonal and interannual scales (Belkin et al., 2007). Most fronts are caused by coastal wind-induced upwelling, which is similar to the Northwest African coastal upwelling (Burton, 1998) and also broadly similar to the upwelling in the California Current (Haynes et al., 1993). The upwelled water gets entrained into large filaments that extend hundreds km offshore. SST fronts are most pronounced during the peak of the upwelling season, from July through September. The wintertime frontal pattern is quite variable from one year to another and depends, at least partially, on the poleward coastal warm current that emerges once the trade winds collapse; this current is however confined to a very narrow near-coastal band, 25-40-km wide; its thermal signature is just 1.0-1.5°C (Belkin et al., 2007).

LME #26: Mediterranean Sea

This LME features a variety of meso-scale fronts that develop seasonally within a particular sea or sub-basin such as the Alboran, Balearic, Ligurian, Tyrrhenian, Ionian, Adriatic, and Aegean seas. The limited horizontal extent of these fronts reflects the extremely complex physiography of the Mediterranean Sea. The following fronts are distinguished here, west to east (Belkin et al., 2007): Almeria-Oran Front (AOF), North Balearic Front (NBF), Ligurian Front (LF), North Tyrrhenian Front (NTF), Sardinia-Sicily Front (SSF), North Adriatic Front (NAF), Albanian Front (AF), Otranto Front (OF), Tunisian Front (TF), Libyan Front (LF), Crete Front (CrF) and Cyprus Front (CyF), as well as some smaller local fronts. Long-term variability of the Mediterranean fronts is substantial as evidenced by a comparison of Figure 26 (Belkin et al., 2007) based on modern data with, e.g., Philippe and Harang (1982).

LME #27: Canary Current

Persistent northerly winds along the coast of Northwest Africa cause a year-round coastal upwelling. The upwelled water is drawn offshore by the Canary Current and also by current jets originated farther south, protruding transversally several hundred km offshore (Barton, 1998; Barton et al., 1998; Progress in Oceanography, 2004, 62(2-4), special issue). These processes create multitude of surface-intensified fronts that develop seasonally, in sync with coastal upwelling. The upwelling zone expands in winter and shrinks in summer and fall. It also migrates meridionally as the season progresses. The zone begins its southern advance in October and reaches its maximum southward extent (5°N) in January-March, then retreats northward, reaching 15°N in late summer (Belkin et al., 2007).

LME #28: Guinea Current

Fronts in the Gulf of Guinea occur mainly off its northern coast, in winter and summer (Belkin et al., 2007). The winter front appears to be the easternmost extension of the coastal Guinea Current that penetrates the Gulf; the front fully develops in January-February, reaching 5°E by March. The summer front emerges largely off Cape Three Points (2°W), usually in July-September, the upwelling season in the Gulf, and sometimes extends quite far offshore, up to 200 km from the coast. The wind-induced upwelling develops east of Cape Palmas (7.5°W) and Cape Three Points owing to the coast's orientation relative to the prevailing winds. Current-induced upwelling and wave propagation also contribute to the observed variability in the Gulf (Ajao and Houghton, 1998).

LME #29: Benguela Current

The coastal upwelling zone off South Africa extends from Cape of Good Hope (34.5°S) north up to 13°S and consists of the two major areas, the northern and southern Benguela upwelling frontal zones, UFZ, separated by the so-called Lüderitz line (LL) at 28°S, where the shelf's width is at minimum (Shannon, 1985; Shillington, 1998). The northern UFZ is year-round, whereas the southern UFZ is seasonal (Belkin et al., 2007). A peculiar double front is observed within the southern UFZ, between 28°S-32°S, with the inshore front close the coast (a few tens km) and the offshore front over the shelf break (150-200 km off the coast). This double-front pattern can be explained by the conceptual model put forth by Barange and Pillar (1992). A vast frontal zone develops seasonally off the Angolan coast. This zone consists of numerous fronts; most fronts extend ESE-WNW; the entire zone seems to protrude seaward from the Angolan coast north of 20°S. This zone is likely related to the Angola-Benguela Front (ABF; Shannon et al., 1987; Meeuwis and Lutjeharms, 1990).

LME #30: Agulhas Current

The Agulhas Current Front (ACF) is the inshore boundary of the very warm and salty Agulhas Current that carries tropical waters past Cape of Good Hope, then retroflects and flows eastward. This front is very deep and stable (within this LME) and is observed year-round. This LME also includes fronts related to the Mozambique Current that flows southward between Africa and Madagascar. The East Madagascar Current Front (EMCF) is observed off southeastern Madagascar, and off the northern tip of Madagascar, where the Glorioso Islands Front (GIF) protrudes northwestward from the namesake islands at 11°30'S, 47°20'E; this front has not been described in the literature until the advent of satellite remote sensing and has been discovered during a global survey of oceanic fronts (Belkin et al., 2007).

LME #31: Somali Coastal Current

The Somali Current develops in sync with the monsoon that dominates the meteorological and hydrographic regime of the Indian Ocean. In summer, the prevailing winds from the southwest accelerate the along-shore Somali Current that flows north, then northeast. North of the equator, the northward Somali Current is deflected eastward, thus resulting in the upwelling of cold, nutrient-rich waters along Somali coast. These waters are separated by a sharp front from the warm and salty waters carried by the Somali Current. With the advent of the winter monsoon, the wind field reverses and the prevailing winds from the northeast shut down the coastal upwelling, spin down the Somali Gyre and cause downwelling along Somali coast (Belkin et al., 2007).

LME #32: Arabian Sea

The Arabian Sea features several fronts, whose development is governed by the seasonal monsoon winds and their reversals. The most stable, seasonally persistent front develops in the Gulf of Aden. This front cuts across the Gulf, from the Arabian Peninsula to Somali coast, with the cross-frontal temperature range up to 5°C. Upwelling fronts are ubiquitous off Pakistan coast and, to a lesser extent, off the western coast of India; these fronts are also seasonal and their development is similar to the seasonal evolution of major upwelling frontal zones off Northwest Africa and off the U.S. West Coast, in the California Current System. A meso-scale front is observed near the entrance to the Persian Gulf (Belkin et al., 2007).

LME #33: Red Sea

The Red Sea has the maximal temperatures and salinities observed in the World Ocean. The extremely high evaporation rate leads to formation of salinity fronts; temperature fronts tend to develop on these salinity fronts. Despite the relative uniformity of meteorological conditions over the Red Sea, fronts emerge owing to wind-induced upwelling, whose effect is accentuated by steep bathymetry and local orographic features. Three groups of fronts are distinguished here, north to south: (1) Egypt-Saudi Arabia Front (ESSF); (2) Sudan-Saudi Arabia fronts (SSAF); and (3) Eritrea-Yemen fronts (EYF). These fronts are poorly studied in situ, whereas satellite observations hold promise thanks to the largely cloud-free conditions over the Red Sea (Belkin et al., 2007).

LME #34: Bay of Bengal

The principal front in the Bay of Bengal is maintained by the huge fresh outflow from the Ganges-Brahmaputra estuary. This is a year-round front, whose cross-frontal TS-ranges vary seasonally. Another estuarine front is maintained by the Irravadi River outflow in the northern Andaman Sea. In both cases the location of estuarine fronts coincides with the shelf break. A front east of Ceylon (Sri Lanka) has been recently described from satellite data (Belkin et al., 2007); its origin is related to the wind-induced upwelling off the east coast of Ceylon. A bathymetrically-trapped front exists along a sill at the northern entrance to the Palk Strait between India and Ceylon.

LME #35: Gulf of Thailand

The only major front within this LME is located near its boundary, at the entrance to the Gulf of Thailand. This front is largely a salinity front between low-salinity waters of the Gulf's proper diluted by the Mekong River outflow, and saline waters of the South China Sea. The salinity contrast between the Gulf waters and South China Sea waters varies seasonally and interannually depending on the Mekong River discharge and can be as high as 3 ppt across the front (Belkin and Cornillon, 2003; Belkin et al., 2007). The attendant thermal front has the cross-frontal range of 2°C to 3°C. The monsoon plays a major role in the front's seasonal evolution since the Mekong River discharge is largely monsoon-dependent; the snowmelt component of the Mekong runoff is of secondary importance.

LME #36: South China Sea

Fronts observed within this LME are quite diverse (Belkin and Cornillon, 2003; Belkin et al., 2007). A major shelf front extends along China coast from Hainan Island into Taiwan Strait; this front separates low-salinity coastal waters from offshore waters. The Bakbo Bay Front is of the estuarine origin; the salinity differential across this front is set up by a massive river discharge into the Bakbo Bay. Fronts off Vietnam coast are largely caused by wind-induced coastal upwelling; their genesis and relaxation depend on the monsoon. A front (or rather a relatively broad frontal zone) southwest of the Luzon Strait is likely caused by the inflow of the Pacific waters; the wind-induced upwelling might also contribute to the front maintenance.

LME #37: Sulu-Celebes Sea

This semi-enclosed sea, like other seas within the Indonesian Archipelago, is connected to the Pacific and Indian Oceans via several straits; flow constriction within these straits is conducive to front formation. The uniformly high surface temperature tends to masks salinity fronts caused by coastal upwelling, whose intensity sharply increases locally owing to orographic and bathymetric effects. Evaporative cooling also contributes to front formation since this process creates a colder and saltier water mass, which is substantially denser than ambient waters (Belkin and Cornillon, 2003; Belkin et al., 2007).

LME #38: Indonesian Sea

Straits connecting this LME with the other marginal seas are sites of front formation due to topographic effects caused by flow constrictions. Internal tide interaction with sills in these straits is one of such front-genetic processes. Local (basin-scale) fronts are observed east of Borneo (EBSSF), northeast of Sulawesi (NESF), east of Halmahera (EHF), in the eastern parts of the Java Sea (EJSF) and Flores Sea (EFSF), across the Makassar Strait (MaSF), in the Molucca Sea (MoSF), and in the southern Banda Sea (SBSF) (Belkin et al., 2007).

LME #39: North Australian Shelf

The main physiographical province within this LME is the Gulf of Carpentaria surrounded by a major seasonal coastal front (Gulf of Carpentaria Front, GCF). The offshore Cape Arnhem Front (CAF) and Cape York Peninsula Front (CYPF) emerge seasonally near the northwest and northeast entrances to the Gulf, respectively. Farther west, the coastal Arafura Sea Front (ASF) is observed north of Arnhem Land, while the coastal Joseph Bonaparte Gulf Front (JBGF) develops in the southern part of the Timor Sea. These fronts are likely to play an important role in the ecology of commercially important prawns (Belkin and Cornillon, 2003; Belkin et al., 2007).

LME #40: Northeast Australian Shelf – Great Barrier Reef

From satellite data (Belkin and Cornillon, 2003; Belkin et al., 2007), the Great Barrier Reef (GBR) is marked by a seasonal thermal front (GBRF) that peaks during the austral winter. This front is better defined off southern Queensland, whereas the fronts' extension off northern Queensland is less robust. Satellite data analysis revealed another, inner shelf front that runs off Queensland coast (QISF). This front appears to consist of three segments, northern, central and southern, whose possible connectivity is not established yet.

LME #41: East-Central Australian Shelf

The westward South Equatorial Current impinges the east coast of Australia and bifurcates, with the two branches flowing in the opposite directions, north and south, along the coast (Belkin and Cornillon, 2003; Belkin et al., 2007). The southward branch is the East Australian Current, a strong western boundary current that carries tropical waters along the entire LME and beyond, into LME #42, eventually down to Tasmania, and is associated with a distinct thermal and salinity front (EACF).

LME #42: Southeast Australian Shelf

The East Australian Current carries tropical waters from LME #41 into LME #42 to feed a southward current associated with the East Bass Strait Front (ESBF). The ESBF extends past the eastern entrance to Bass Strait, along Tasmania's east cost, and finally turns east. This front is the strongest during the austral winter and still distinct in summer when its cross-frontal range is about 1°C. The Subtropical Front (STF) continues eastward along the shelf edge toward Tasmania. The Kangaroo Island Front (KIF) develops seasonally SE of Kangaroo Island caused by wind-driven coastal upwelling (Belkin and Cornillon, 2003; Belkin et al., 2007).

LME #43: Southwest Australian Shelf

The warm and saline Leeuwin Current (originated within LME #44) rounds Cape Leeuwin to enter the Great Australian Bight. The Leeuwin Current and the associated TS-front (Leeuwin Current Extension Front, LCEF) continue eastward generally along the shelf edge all the way up to Spencer Gulf. An estuarine front exists across the entrance to Spencer Gulf (SGF). Two inner shelf/near-coastal fronts are observed in the western and eastern parts of the Great Australian Bight (WGABF and EGABF) (Belkin and Cornillon, 2003; Belkin et al., 2007).

LME #44: West-Central Australian Shelf

The Leeuwin Current Front (LCF) originates within this LME, although some source waters of this current/front are found farther north, in LME #45 (Belkin et al., 2007). Tropical warm, salty waters spread along this front toward Cape Leeuwin. The North Tropical Front (NTrF) merges with the LCF near 25°S. Farther south, the South Tropical Front (STrF) merges the LCF near 30°S. The LCF and the associated current extend over the shelf break and shelf. They play an important role in ecology of many tropical species, particularly lobster, since the Leeuwin Current and its extension carry lobster eggs and larvae into the Great Australian Bight. A meso-scale Kalbarri Inner Shelf Front (KISF) extends NNW from the Murchison River mouth at 27.5°S.

LME #45: Northwest Australian Shelf

This vast shelf is a source area of the Leeuwin Current that flows along the west coast of Australia carrying warm and salty tropical waters far south. Seasonal evolution of frontal pattern over this shelf is somewhat similar to that west of Northwest Africa and west of the U.S. West Coast. In summer, multitude of small-scale fronts develops that form a chaos-like spatial pattern. As the seasons progresses, these small-scale fronts apparently coalesce into large-scale (hundreds km long) coherent filaments that persist for weeks and months. Tidal mixing over this shelf deems important, although no stable tidal mixing fronts have been detected within this LME (Belkin et al., 2007).

LME #46: New Zealand Shelf

This LME features several well-defined fronts that together determine the ecological regime of the New Zealand shelf (Belkin and Cornillon, 2003). In the north, the Tasman Front and its extension associated with the North Cape Current bring warm and salty tropical waters to the east coast of North Island. This influx, together with vigorous tidal mixing thanks to rough bathymetry, are largely responsible for the exceptionally high productivity off the Bay of Islands , where big game fish like marlins and kingfish come unusually close to the mainland coast, forming fishing grounds just a few miles offshore, e.g. off Cape Brett. West of North Island, the southern branch of the Tasman Front heads toward Cook Strait. In the south, the Southland Current Front runs northward along the east coast of South Island toward Banks Peninsula. East of New Zealand, the double Subtropical Frontal Zone extends eastward along the north and south flanks of the Chatham Rise up to Chatham Island and beyond.

LME #47: East China Sea

This LME features diverse fronts (Hickox et al., 2000; Belkin and Cornillon, 2003). In the north, the Yangtze Bank Ring Front (YBRF) surrounds the Yangtze Bank (Shoal). This front is caused by the huge fresh discharge of the Yangtze River and is maintained by tidal rectification that results in a clockwise current (and a closed quasi-circular front) around the Bank. A water mass front (FZF) exists along the Fujian-Zhejiang Coast between warm, saline waters flowing northward via Taiwan Strait and cold, fresh waters flowing southward along the coast. The Kuroshio Front (KF) invades the shelf north of Taiwan. These excursions are important for the cross-shelf exchange of heat, salt and nutrients. Sharp fronts exist between warm, saline waters of the Kuroshio and Taiwan Strait that flow northward-northeastward and colder, fresher coastal waters off Cheju Island in Tsushima (Korea) Strait that flow southwestward (CIF).

LME #48: Yellow Sea

Several tidal mixing fronts exist within this LME that includes the Yellow Sea and Bohai Sea (Hickox et al., 2000; Belkin and Cornillon, 2003). The most conspicuous fronts are observed around Shandong Peninsula (between Yellow Sea and Bohai Sea), off Jiangsu Shoal, and off two major bays west of Korean Peninsula. A new front identified in Bohai Sea (Hickox et al., 2000) is likely a water mass front between waters that flow in and out of the Bohai Sea. The freshwater discharge of the Yellow River plays a minor role in maintaining the Yellow Sea fronts compared with the Yangtze River discharge's role in maintaining the East China Sea fronts (LME #47). A subsurface front in the central part of the Yellow Sea surrounds cold water mass formed by wintertime cold air outbreaks.

LME #49: Kuroshio Current

The Kuroshio Current is associated with two parallel fronts (Belkin and Cornillon, 2003). The strongest front exists along the inshore boundary of the Kuroshio Current, whereas a weaker front is observed along the Kuroshio's offshore boundary. This double Kuroshio Front (KF) forms a large meander off Japan, downstream of Izu Ridge. This meander emerges and disappears quasi-periodically. Its emergence is linked to interannual fluctuations in the Kuroshio transport and is ultimately related to the Pacific Decadal Oscillation (PDO) and El-Nino-Southern Oscillation (ENSO). The Kuroshio Front leaves the coast of Japan off Cape Inubo where it forms two quasi-stationary meanders, the so-called First and Second Meanders of the Kuroshio. These meanders often spawn extremely energetic anticyclonic warm-core rings that exist for many months in a transition zone between the Kuroshio Front and the Oyashio Front (OF)(Belkin et al., 2007).

LME #50: Sea of Japan

The Subarctic (Subpolar) Front (SAF) crosses the Japan (East) Sea zonally west to east and then extends meridionally northward into the Gulf of Tartar (Tatarskiy Zaliv). From satellite data, three tributaries of this front have been identified in the western part of the sea (Belkin and Cornillon, 2003). This major front divides the Japan Sea into two parts, northern and southern, with different oceanographic regimes. The Liman Current Front (LCF) extends along a coast of the Russian Far Eastern province Primorskii Krai in the northwestern part of the Japan Sea. Small and meso-scale fronts are generated near Laperouse Strait and in the southern part of the Gulf of Tartar owing to vigorous tidal mixing and influx of the Okhotsk Sea waters.

LME #51: Oyashio Current

The Oyashio Current Front originates at the western periphery of the Western Subarctic Gyre. The upstream part of the Oyashio Current/Front is also called the East Kamchatka Current/Front and Kuril Current/Front (Belkin and Cornillon, 2003). The Oyashio Current carries cold and fresh waters southwestward where they meet warm and salty waters of the Kuroshio. As it flows southwestward, the Oyashio Current forms energetic eddies, up to 50-100 km in diameter, branches into the Okhotsk Sea via the Kuril Straits and undergoes water mass transformation owing to extremely intense tidal mixing in the Kuril Straits. A major permanent branch of the Oyashio Current penetrates into the Okhotsk Sea to form the West Kamchatka Current.

LME #52: Sea of Okhotsk

This LME is characterized by a very energetic tidal regime and intense water mass exchange with the open Pacific Ocean; as a result, several fronts of various physical natures exist here (Belkin and Cornillon, 2003, 2004). A branch of the Kamchatka Current penetrates into the Okhotsk Sea via the First Kuril Strait to form the West Kamchatka Current associated with a water mass front (WKCF). Robust tidal mixing fronts develop over the western and northern shelves (WSF and NSF, respectively), especially off Magadan (MSF) and within Shelikhov Gulf (SGF), where the tidal magnitude peaks at 12 to 13 m. Very sharp tidal mixing front surround Kashevarov Bank (KBF) and Shantarsky Islands. An estuarine front bounds the Amur River plume; this front continues southward along the east coast of Sakhalin as the East Sakhalin Current Front (ESCF).

LME #53: West Bering Sea

A major northwestward current of the Eastern and Western Bering Sea shelves bifurcates upstream of Cape Navarin. The northward branch flows toward Bering Strait as the Anadyr-Chukotka Current associated with the Gulf of Anadyr Front (GAF). The southward branch flows first along the Koryak Coast, then along Kamchatka Peninsula, and is associated respectively with the Koryak Coast Current Front (KCCF) and the East Kamchatka Current Front (EKCF). The KCCF is very stable, apparently owing to a very steep upper continental slope and well defined sharp shelf break off Koryak Coast that together steer this front (Belkin and Cornillon, 2003). The East Kamchatka Current is by far the most important flow out of the Bering Sea, exporting over 10^7 m^3/s of cold, low-salinity water.

LME #54: Chukchi Sea

Five fronts are found within this LME (Belkin et al., 2003). The Kotzebue Sound Front (KSF) bounds the northward Bering inflow. Low-salinity Bering Sea waters flow around Chukotka northwestward along the Chukotka Front (CF) toward Herald Valley. The Siberian Coastal Current/Front (SCCF) enters the Chukchi Sea through Long Strait, rounds Wrangel Island and continues northward via Herald Valley. The Herald Shoal Front (HSF) is situated over the steep southern slope of the namesake shoal. A stable front extends along Barrow Canyon (BCF).

LME #55: Beaufort Sea

The Shelf Break/Shelf-Slope Front (SSF) is the most robust front within this LME. Its stability depends on the steepness of the upper continental slope. Accordingly, this front is the most stable where the shelf break is best defined and the slope is the steepest, namely off Cape Bathurst in the Canadian Beaufort Sea (Belkin et al., 2003). This place is well known as the site of Cape Bathurst Polynya and also a “hot spot” of marine life where sea birds and marine mammals congregate. Transient fronts form at the dynamic boundary of the Mackenzie River plume and also within this plume.

LME #56: East Siberian Sea

The Siberian Coastal Current (SCC) is associated with a front (SCCF) that extends across the southern part of this LME. The front separates low-salinity coastal waters from offshore waters. The SCC carries huge amount of fresh water from great Siberian rivers such as Ob', Yenisey and Lena, and also Khatanga, Olenek, Indigirka, Yana, and Kolyma. The SCC transports these waters along the SCCF eastward through Long Strait into the Chukchi Sea. Estuarine fronts develop off the mouths of Indigirka and Kolyma, and also off Ayon Island.

LME #57: Laptev Sea

This area features a huge river runoff owing primarily to the Lena River discharge, and also discharges of the Khatanga (merger of Kheta and Kotuy), Popigay, Anabar, Olenek, and Yana rivers. Estuarine offshore fronts develop as freshwater river plumes formed by Lena and Khatanga spread over the vast shallow shelf of Laptev Sea. Similar to the Mackenzie River plume, these plumes may contain multiple transient fronts that correspond to individual freshets. The Siberian Coastal Current Front is less distinct in Laptev Sea compared to the East Siberian and Chukchi seas. This front separates low-salinity inshore waters from saltier offshore waters and acts as a conduit for the fresh waters on their route eastward. The Laptev Sea continental slope is relatively steep and the shelf break is well defined, therefore a shelf-slope front might exist along the shelf edge.

LME #58: Kara Sea

The Ob' and Yenisey River discharges to the Kara Sea form a giant single freshwater plume since both estuaries are close to each other. This plume spreads across the entire Kara Sea, up to Novaya Zemlya. The distribution of this plume is largely determined by the wind field that is ultimately by large-scale atmospheric pressure pattern. Sharp salinity and temperature fronts are observed in outer parts of Ob' and Yenisey's estuaries called Obskaya Guba and Yeniseyskiy Zaliv, respectively, where riverine waters meet oceanic waters. In the southwestern part of the Kara Sea, a front exists between resident waters and the Atlantic inflow from the Barents Sea through Karskiye Vorota, a strait that connects the Kara Sea with the Pechora Sea, a southeastern extension of the Barents Sea.

LME #59: Iceland Shelf

The Irminger Current's warm and salty waters arrive to the Iceland Shelf from the south and circulate anticyclonically (clockwise) around Iceland. The Polar and Arctic waters, both relatively fresh and cold, arrive from the north to meet the Irminger waters over the Iceland Shelf where two major fronts form. The Irminger Current-West Iceland Front (ICWIF) is located where the Irminger waters meet the western branch of cold, fresh waters heading toward the Denmark Strait. The North Iceland Front (NIF) is located north and northeast of Iceland where the North Icelandic Current meets the eastern branch of the Irminger-Icelandic Current (Belkin et al., 2007). The North Iceland Front appears to be connected to the Iceland-Faroes Front (IFF) observed farther east.

LME #60: Faroe Plateau

The Faroe Plateau is surrounded by tidal mixing fronts (Belkin et al., 2007). These fronts define the Plateau ecosystem and its important fishery grounds, especially herring and cod. Unlike their counterparts around British Isles, the Faroese tidal mixing fronts have not been studied in detail. A large-scale water mass front between the Plateau waters and the North Atlantic waters exists at the boundary of this LME, running along the Faroe-Shetland Channel (Belkin et al., 2007).

LME #61: Antarctic

The Antarctic Shelf-Slope Front (ASSF) is observed along most of the Antarctic shelf/slope, except for the southern Pacific Antarctic and also a part of the Weddell Sea. This front separates very cold shelf waters from warmer oceanic waters. A geostrophic current that flows westward along this front carries icebergs around the continent for thousands of kilometers, branching north into marginal Antarctic seas. This current and associated front is largely set up by strong and persistent katabatic winds that drain very cold air from the Antarctic Plateau. Local fronts exist off the Antarctic Peninsula, in the Prydz Bay, and in the Ross Sea (Belkin et al., 2007).

LME #62: Black Sea

A major front has been recently described from satellite data that extends along the 50-m isobath from Cape Tarhankut (Crimean Peninsula) southwestward toward Bulgarian Coast, with the cross-frontal surface temperature step of up to 4°C and salinity step of up to 1 ppt (Belkin et al., 2007). This front develops in winter and peaks in February-March. Another large-scale front is associated with the Rim Current that flows around the Black Sea. Even though this front largely follows the shelf edge, it is less robust because the Rim Current meanders and spawns eddies and rings. Estuarine fronts off the Dnieper and Dniester River mouths and off the Danube River delta are expected, as well as a front off Kerch Strait that connects the Azov Sea and Black Sea; these fronts have not been studied in detail.

LME #63: Hudson Bay

This LME appears relatively uniform as it features just a few comparatively weak fronts, mainly around its periphery. The most robust thermal front is observed in the far south, within James Bay, probably related to the enhanced freshwater discharge into the apex of James Bay that generates a collocated salinity front. Similar estuarine fronts are likely to exist elsewhere off the Bay's eastern, southern and western shores, peaking after spring freshets. A meandering front develops in the northern part of Hudson Bay between waters that flow into the Bay from the northwest and resident waters. This front develops seasonally; its location and TS-characteristics ultimately depend on the seasonal ice cover melt since the latter determines the amount of fresh water released by the melting sea ice and eventually determines the salinity differential across this front.

LME #64: Arctic Ocean

Numerous fronts are observed in the Arctic marginal seas described in LME ## 18-20 and 54-58. Observations of fronts in the open Arctic Ocean are hampered by perennial ice cover that prevents satellite remote sensing of fronts in the Arctic Basin. Hydrographic surface and subsurface data collected from surface vessels, ice drifting stations and submarine revealed a major front in the central Arctic that separates Atlantic waters from Pacific waters. Until the mid-1990s, this front was located over Lomonosov Ridge (LRF). Observations from the late 1990s and early 2000s have documented a major shift of this front that occurred around 1995. Since then, the front ran along Mendeleyev-Alpha Ridge (MARF). In is unclear yet if the front will shift back in the future and if such shifts occurred in the past.

4. Summary

Frontal patterns in 64 World Ocean’s Large Marine Ecosystems have been determined from 12 years, 1985-1996, of satellite 9-km global AVHRR SST fields processed with the Cayula-Cornillon front detection algorithm. Several major frontal types have been distinguished that can be reliably monitored from remote sensing data, e.g. tidal mixing fronts; estuarine, river plume, shelf, shelf-break and shelf-slope fronts; coastal and equatorial upwelling fronts; subtropical convergence fronts; western and eastern boundary currents; and marginal ice zone fronts. Stationary fronts are steered by topography and therefore are most stable but not necessarily feature largest horizontal gradients of properties. Most thermal fronts are collocated with chlorophyll fronts (Belkin and O’Reilly, 2007), suggesting causative links between these two types of fronts.

Acknowledgments. We are grateful to NASA, NOAA and UNEP for supporting this study since 1998 till present. Numerous discussions with Ken Sherman and Jay O’Reilly were most helpful. Dave Ullman’s assistance with the front detector algorithm and data processing was indispensable.

5. References

Ajao, E. A. and R. W. Houghton (1998) Coastal ocean of Equatorial West Africa from 10°N to 10°S, in: *The Sea, vol. 11: The Global Coastal Ocean, Regional Studies and Syntheses*, edited by A. R. Robinson and K. H. Brink, pp. 605-630, John Wiley and Sons, New York etc.

Atkinson, L. P. and D. W. Menzel (1985) Introduction: Oceanography of the Southeastern United States Continental Shelf, in: *Oceanography of the Southeastern U.S. Continental Shelf*, edited by L. P. Atkinson, D. W. Menzel, and K. A. Bush, pp. 1-9, Coastal and Estuarine Sciences, vol. 2, American Geophysical Union, Washington, D.C.

Barange, M., and S. C. Pillar (1992) Cross-shelf circulation, zonation and maintenance mechanisms of *Nyctiphanes capensis* and *Euphausia hanseni* (Euphausiacea) in the northern Benguela upwelling system, *Cont. Shelf Res.*, *12*(9), 1027-1042.

Barton, E. D. (1998) Eastern boundary of the North Atlantic: Northwest Africa and Iberia, in *The Sea, vol. 11: The Global Coastal Ocean, Regional Studies and Syntheses*, edited by A. R. Robinson and K. H. Brink, pp. 633-658, John Wiley and Sons, New York etc.

Barton, E. D. et al. (1998) The transition zone of the Canary Current upwelling region, *Progr. Oceanogr.*, *41*(4), 455–504.

Belkin, I.M. (1993) Frontal structure of the South Atlantic, in *Pelagic Ecosystems of the Southern Ocean*, edited by N. M. Voronina, pp. 40-54 (in Russian), Nauka Press, Moscow.

Belkin, I.M. (2003) Front, in: *Interdisciplinary Encyclopedia of Marine Sciences*, edited by J. W. Nybakken, W. W. Broenkow, and T. L. Vallier, pp. 433-436, Grolier Academic Reference, Danbury, Connecticut.

Belkin, I.M. (2004) Propagation of the “Great Salinity Anomaly” of the 1990s around the northern North Atlantic, *Geophys. Res. Lett.*, **31**, L08306, doi:10.1029/2003GL019334.

Belkin, I.M. (2005) Oceanic Fronts in Large Marine Ecosystems, Final Report to the United Nations Environment Programme, 49 pp., 64 maps.

Belkin, I. M., and P. C. Cornillon (2003) SST fronts of the Pacific coastal and marginal seas, *Pacific Oceanography*, *1*(2), 90-113.

Belkin, I. M., and P. C. Cornillon (2004) Surface thermal fronts of the Okhotsk Sea, *Pacific Oceanography*, *2*(1-2), 6-19.

Belkin, I. M., and P. C. Cornillon (2005) Bering Sea thermal fronts from Pathfinder data: Seasonal and interannual variability, *Pacific Oceanography*, *3*(1), 6-20.

Belkin, I.M., and J.E. O'Reilly (2007) New algorithm for oceanic front detection in chlorophyll and sea surface temperature satellite imagery, *J. Marine Systems*, submitted.

Belkin, I.M., P. Cornillon, and D. Ullman (2003) Ocean fronts around Alaska from satellite SST data, Proceedings of the Amer. Met. Soc. 7th Conf. on the Polar Meteorology and Oceanography, Hyannis, MA, Paper 12.7, 15 pp.

Belkin, I.M., P.C. Cornillon, D.S. Ullman and Z. Shan (2007) Global survey of oceanic fronts from Pathfinder SST data: I. Atlantic Ocean, II. Pacific Ocean, III. Indian Ocean (to be submitted to *Progress in Oceanography*).

Belkin, I.M., and A.L. Gordon (1996) Southern Ocean fronts from the Greenwich meridian to Tasmania, *J. Geophys. Res.*, *101*(C2), 3675-3696.

Belkin, I.M. and S. Levitus (1996) Temporal variability of the Subarctic Front near the Charlie-Gibbs Fracture Zone, *J. Geophys. Res.*, *101*(C12), 28317-28324.

Belkin, I.M., S. Levitus, J.I. Antonov, and S.-A. Malmberg (1998) "Great Salinity Anomalies" in the North Atlantic, *Progress in Oceanography*, *41*(1), 1-68.

Campos, E. J. D., J. E. Gonçalves, and Y. Ikeda (1995) Water mass characteristics and geostrophic circulation in the Southern Brazil Bight: Summer of 1991, *J. Geophys. Res.*, *100*(C9), 18,537-18,550.

Campos, E. J. D., C. A. D. Lentini, J. L. Miller, and A. R. Piola (1999) Interannual variability of the sea surface temperature in the South Brazil Bight, *Geophys. Res. Lett.*, *26* (14), 2061-2064.

Cayula, J.-F., and P. Cornillon (1992) Edge detection algorithm for SST images, *J. Atm. Oc. Tech.*, *9*(1), 67-80.

Cayula, J.-F., and P. Cornillon (1995) Multi-image edge detection for SST images. *J. Atm. Oc. Tech.*, *12*(4), 821-829.

Cayula, J.-F., and P. Cornillon (1996) Cloud detection from a sequence of SST images, *Rem. Sens. Envir.*, *55*(1), 80-88.

Cayula, J.-F., P. Cornillon, R. Holyer, and S. Peckinpaugh (1991) Comparative study of two recent edge-detection algorithms designed to process sea-surface temperature fields, *IEEE Trans. Geosci. Rem. Sens.*, *29*(1), 175-177.

Ciotti, Á. M., C. Odebrecht, G. Fillmann, and O. O. Möller, Jr. (1995) Freshwater outflow and Subtropical Convergence influence on phytoplankton biomass on the southern Brazilian continental shelf, *Cont. Shelf Res.*, *15*(14), 1737-1756.

Haynes, R., E. D. Barton, and I. Pilling (1993) Development, persistence, and variability of upwelling filaments off the Atlantic coast of the Iberian Peninsula, *J. Geophys. Res.*, *98* (C12), 22681-22692.

Heyman, W. D., and B. Kjerfve (1999) Hydrological and oceanographic considerations for integrated coastal zone management in southern Belize, *Environ. Management*, *24*(2), 229-245.

Hickey, B. M. (1998) Coastal oceanography of western North America from the tip of Baja to Vancouver Island, in: *The Sea, The Global Coastal Ocean: Regional Studies and Syntheses, vol. 11*, edited by A. R. Robinson and K. H. Brink, Wiley, New York, pp. 345-393.

Hickox, R., I.M. Belkin, P. Cornillon, and Z. Shan (2000) Climatology and seasonal variability of ocean fronts in the East China, Yellow and Bohai Seas from satellite SST data, *Geophys. Res. Lett.*, *27*(18), 2945-2948.

Huh, O. K., W. J. Wiseman, Jr., and L. J. Rouse, Jr. (1978) Winter cycle of sea surface thermal patterns, northeastern Gulf of Mexico, *J. Geophys. Res.*, *83*(C9), 4523-4529.

Lima, I. D., and J. P. Castello (1995) Distribution and abundance of South-west Atlantic anchovy spawners (*Engraulis anchoita*) in relation to oceanographic processes in the southern Brazilian shelf, *Fish. Oceanogr.*, *4*(1), 1-16.

Lima, I. D., C. A. E. Garcia, and O. O. Möller (1996) Ocean surface processes on the southern Brazilian shelf: characterization and seasonal variability, *Cont. Shelf Res.*, *16*(10), 1307-1317.

Linder, C. A., and G. Gawarkiewicz (1998) A climatology of the shelfbreak front in the Middle Atlantic Bight, *J. Geophys. Res.*, *103*(C9), 18,405-18,423.

Mavor, T. P., and J. J. Bisagni (2001) Seasonal variability of sea-surface temperature fronts on Georges Bank, *Deep-Sea Res. II*, *48*(1-3), 215-243.

Meeuwis, J. M., and J. R. E. Lutjeharms (1990) Surface thermal characteristics of the Angola-Benguela front, *S. Afr. J. Mar. Sci.*, *9*, 261-279.

Philippe, M., and L. Harang (1982) Surface temperature fronts in the Mediterranean Sea from infrared satellite imagery, in: *Hydrodynamics of Semi-Enclosed Seas*, edited by J.C.J. Nihoul, pp. 91-128, Elsevier, New York.

Pietrafesa, L. J., G. S. Janowitz, and P. A. Wittman (1985) Physical oceanographic processes in the Carolina Capes, in: *Oceanography of the Southeastern U.S. Continental Shelf*, edited by L. P. Atkinson, D. W. Menzel, and K. A. Bush, pp. 23-32, Coastal and Estuarine Sciences, vol. 2, AGU, Washington, DC.

Piola, A. R., E. J. D. Campos, O. O. Miller Jr., J. Charo, and C. Martinez (2000) Subtropical shelf front off eastern South America, *J. Geophys. Res.*, *105*(C3), 6565–6578.

Shannon, L. V., editor (1985) *South African Ocean Colour and Upwelling Experiment*, Sea Fisheries Research Institute, Cape Town, 270 pp.

Shannon, L. V., J. J. Agenbag, and M. E. L. Buys (1987) Large- and mesoscale features of the Angola-Benguela Front, *S. Afr. J. Mar. Sci.*, *5*, 11-34.

Shillington, F. A. (1998) The Benguela upwelling system off Southwestern Africa, in: *The Sea, vol. 11: The Global Coastal Ocean, Regional Studies and Syntheses*, edited by A. R. Robinson and K. H. Brink, pp. 583-604, John Wiley and Sons, New York etc.

Ullman, D. S. and P. C. Cornillon (1999) Surface temperature fronts off the East Coast of North America from AVHRR imagery, *J. Geophys. Res.*, *104*(C10), 23,459-23,478.

Ullman, D. S. and P. C. Cornillon (2000) Evaluation of front detection methods for satellite-derived SST data using in situ observations, *J. Atm. Oceanic Tech.*, *17*(12), 1667-1675.

Ullman, D. S. and P. C. Cornillon (2001) Continental shelf surface thermal fronts in winter off the northeast US coast, *Cont. Shelf Res.*, *21*(11-12), 1139-1156.

Vazquez, J., K. Perry, and K. Kilpatrick (1998) NOAA/NASA AVHRR Oceans Pathfinder Sea Surface Temperature Data Set User's Reference Manual, Version 4.0, JPL Publication D-14070; also available on the Web: http://podaac.jpl.nasa.gov/pub/sea_surface_temperature/avhrr/pathfinder/doc/usr_gde4_0.html

Figure Captions in Plates 1-4

Figure 1. Fronts of LME #01 (Eastern Bering Sea). Acronyms: **BBF**, Bristol Bay Front; **ISF**, Inner Shelf Front; **KBF**, Kuskokwim Bay Front; **MSF**, Mid-Shelf Front; **OSF**, Outer Shelf Front; **PF**, Polar Front; **SSF**, Shelf-Slope Front; **SSNSF**, Shpanberg Strait-Norton Sound Front. Yellow line, LME boundary.

Figure 2. Fronts of LME #02 (Gulf of Alaska). Acronyms: **IPF**, Inner Passage Front; **KF**, Kodiak Front; **PF**, Polar Front; **SSF**, Shelf-Slope Front (most probable location). Yellow line, LME boundary.

Figure 3. Fronts of LME #03 (California Current). Acronyms: **CCF**, California Current Front; **DCF**, Davidson Current Front (winter only); **SAF**, Subarctic Front; **SSF**, Shelf-Slope Front (most probable location). Yellow line, LME boundary.

Figure 4. Fronts of LME #04 (Gulf of California). Acronyms: **IGF**, Inner Gulf Front; **OGF**, Outer Gulf fronts; **SSF**, Shelf-Slope Front (most probable location). Yellow line, LME boundary.

Figure 5. Fronts of LME #05 (Gulf of Mexico). Acronyms: **CBCF**, Campeche Bank Coastal Front; **CBSSF**, Campeche Bank Shelf-Slope Front (most probable location); **ISF**, Inner Shelf Front; **LCF**, Loop Current Front; **LTSF**, Louisiana-Texas Shelf Front; **MRE**, Mississippi River Estuary; **WFSF**, West Florida Shelf Front. Yellow line, LME boundary.

Figure 6. Fronts of LME #06 (Southeast U.S. Continental Shelf). Acronyms: **CB**, Charleston Bump; **IGSF**, Inshore Gulf Stream Front; **MSF**, Mid-Shelf Front; **OGSF**, Offshore Gulf Stream Front. Yellow line, LME boundary.

Figure 7. Fronts of LME #07 (Northeast U. S. Continental Shelf). Acronyms: **CCF**, Cape Cod Front; **GBF**, Georges Bank Front; **MCF**, Maine Coastal Front; **MSF**, Mid-Shelf Front; **NSF**, Nantucket Shoals Front; **SSF**, Shelf-Slope Front. Yellow line, LME boundary.

Figure 8. Fronts of LME #08 (Scotian Shelf). Acronyms: **CNF**, Cape North Front; **CSF**, Cabot Strait Front (most probable location); **GF**, Gully Front; **SSF**, Shelf-Slope Front. Yellow line, LME boundary.

Figure 9. Fronts of LME #09 (Newfoundland-Labrador Shelf). Acronyms: **FCF**, Flemish Cap Front; **LMSF**, Labrador Mid-Shelf Front; **LSSF**, Labrador Shelf-Slope Front. Yellow line, LME boundary.

Figure 10. Fronts of LME #10 (Insular Pacific-Hawaiian). Acronyms: **STF**, Subtropical Front. Yellow line, LME boundary.

Figure 11. Fronts of LME #11 (Pacific Central-American Coastal). Acronyms: **CR**, Costa Rica; **CRF**, Costa Rica Front; **EGPF**, East Gulf of Panama Front; **ES**, El Salvador; **GTF**, Gulf of

Tehuantepec Front; **GUAT**, Guatemala; **NIC**, Nicaragua; **SSF**, Shelf-Slope Front (most probable location); **WGPF**, West Gulf of Panama Front. Yellow line, LME boundary.

Figure 12. Fronts of LME #12 (Caribbean Sea). Acronyms: **BF**, Belize Front; **DOM. REP.**, Dominican Republic; **EVF**, East Venezuela Front; **GVF**, Gulf of Venezuela Front; **IGBBF**, Inner Great Bahama Bank Front; **JHF**, Jamaica-Haiti Front; **NCF**, North Colombia Front; **OGBBF**, Outer Great Bahama Bank Front; **PR**, Puerto Rico (U.S.); **SECF**, Southeast Cuba Front; **SJF**, South Jamaica Front; **SWCF**, Southwest Cuba Front; **WPF**, Windward Passage Front; **WVF**, West Venezuela Front. Yellow line, LME boundary.

Figure 13. Fronts of LME #13 (Humboldt Current). Acronyms: **CSSF**, Chilean Shelf-Slope Front (most probable location); **NF**, Nazca Front; **NSTF**, North Subtropical Front; **PUF**, Peruvian Upwelling Front; **SSTF**, South Subtropical Front. Yellow line, LME boundary.

Figure 14. Fronts of LME #14 (Patagonian Shelf). Acronyms: **BBF**, Bahia Blanca Front; **BGF**, Bahia Grande Front; **FMCF**, Falkland/Malvinas Current Front; **LPF**, La Plata Front; **MSF**, Mid-Shelf Front; **PMF**, Patagonian-Magellan Front; **SJF**, San Jorge Front; **TFF**, Tierra del Fuego Front; **VF**, Valdes Front.

Figure 15. Fronts of LME # 15 (South Brazil Shelf). Acronyms: **SSF**, Shelf-Slope Front. Yellow line, LME boundary.

Figure 16. Fronts of LME #16 (East Brazil Shelf). Acronyms: **NBCF**, North Brazil Current Front; **SBCF,** South Brazil Current Front; **SSF**, Shelf-Slope Front (most probable location). Yellow line, LME boundary.

Figure 17. Fronts of LME #17 (North Brazil Shelf). Acronyms: **NBCF**, North Brazil Current Front; **SSF**, Shelf-Slope Front (most probable location). Yellow line, LME boundary.

Figure 18. Fronts of LME #18 (West Greenland Shelf). Acronyms: **MSF**, Mid-Shelf Front (most probable location); **WGCF**, West Greenland Current Front. Yellow line, LME boundary.

Figure 19. Fronts of LME #19 (East Greenland Shelf). Acronyms: **EGPF**, East Greenland Polar Front; **MSF**, Mid-Shelf Front (most probable location). Yellow line, LME boundary.

Figure 20. Fronts of LME #20 (Barents Sea). Acronyms: **PF**, Polar Front; **KF**, Kola Front. Yellow line, LME boundary.

Figure 21. Fronts of LME #21 (Norwegian Sea). Acronyms: **AF**, Arctic Front; **IFF,** Iceland-Faroes Front; **NACF,** North Atlantic Current Front; **NCCF,** Norwegian Coastal Current Front. Yellow line, LME boundary.

Figure 22. Fronts of LME #22 (North Sea). Acronyms: **CF**, Central Front; **DBF**, Dogger Bank Front; **EECF**, East English Channel Front; **FF**, Frisian Front; **FHF**, Flamborough Head Front; **FIF**, Fair Isle Front; **NCCF**, Norwegian Coastal Current Front; **ShF**, Shetland Front; **SkF**, Skagerrak Front; **WECF**, West English Channel Front. Yellow line, LME boundary.

Figure 23. Fronts of LME #23 (Baltic Sea). Acronyms: **AF**, Arkona Front; **BBF**, Bothnian Bay Front; **BSF**, Bothnian Sea Front; **GF**, Gotland Front; **ISF**, Irbe Strait Front; **NBPF**, North Baltic Proper Front; **SBPF,** South Baltic Proper Front; **WF**, Western Front (most probable location).

Figure 24. Fronts of LME #24 (Celtic-Biscay Shelf). Acronyms: **IF**, Irish Front; **MSF**, Mid-Shelf Front; **SSF**, Shelf-Slope Front; **UF**, Ushant Front. Yellow line, LME boundary.

Figure 25. Fronts of LME #25 (Iberian Coastal). Acronyms: **SSF**, Shelf-Slope Front. Yellow line, LME boundary.

Figure 26. Fronts of LME #26 (Mediterranean Sea). Acronyms, fronts: **AF**, Albanian Front; **AOF**, Almeria-Oran Front; **CrF**, Crete Front; **CyF**, Cyprus Front; **LbF**, Libyan Front; **LgF**, Ligurian Front; **NAF**, North Adriatic Front; **NBF**, North Balearic Front; **NTF**, North Tyrrhenian Front; **OF**, Otranto Front; **SSF**, Sardinia-Sicily Front; **TF**, Tunisian Front. Acronyms, countries: **BH**, Bosnia-Herzegovina; **CR**, Croatia; **IS**, Israel; **LE**, Lebanon; **MO**, Montenegro; **SL**, Slovenia; **SY**, Syria.

Figure 27. Fronts of LME #27 (Canary Current). Acronyms: **SSF**, Shelf-Slope Front. Yellow line, LME boundary.

Figure 28. Fronts of LME #28 (Guinea Current). Acronyms: **EF**, Equatorial Front; **SSF**, Shelf-Slope Front (solid line, well-defined path; dashed line, most probable location). Yellow line, LME boundary.

Figure 29. Fronts of LME #29 (Benguela Current). Acronyms: **ABF**, Angola-Benguela Front; **LL**, Lüderitz line; **SSF**, Shelf-Slope Front. Yellow line, LME boundary.

Figure 30. Fronts of LME #30 (Agulhas Current). Acronyms: **AB**, Agulhas Bank; **ACF**, Agulhas Current Front; **EMadCF**, East Madagascar Current Front; **GIF**, Glorioso Islands Front; **IACF**, Inshore Agulhas Current Front; **MozCF**, Mozambique Channel fronts; **MozSSF**, Mozambique Shelf-Slope Front; **OACF**, Offshore Agulhas Current Front; **WMadSSF**, West Madagascar Shelf-Slope Front (most probable location). Yellow line, LME boundary.

Figure 31. Fronts of LME #31 (Somali Coastal Current). Acronyms: **EAF**, East African Front; **SCF**, Somali Current Front; **SEF**, South Equatorial Front. Yellow line, LME boundary.

Figure 32. Fronts of LME #32 (Arabian Sea). Acronyms: **GAF**, Gulf of Aden Front; **GOF**, Gulf of Oman Front; **IEF**, Indus Estuarine Front; **OCF**, Oman Coastal Front; **PGF**, Persian Gulf Front; **WIMSF**, West Indian Mid-Shelf fronts; **WISSF**, West Indian Shelf-Slope Front (most probable location). Yellow line, LME boundary.

Figure 33. Fronts of LME #33 (Red Sea). Acronyms: **ESSF**, Egypt-Saudi Arabia Front; **EYF**, Eritrea-Yemen fronts; **SSAF**, Sudan-Saudi Arabia fronts. Yellow line, LME boundary.

Figure 34. Fronts of LME #34 (Bay of Bengal). Acronyms: **ECF**, East Ceylon Front; **GBEF**, Ganges-Brahmaputra Estuarine Front; **IEF**, Irravadi Estuarine Front; **MSSF**, Myanmar Shelf-Slope Front; **PSF**, Palk Strait Front; **TSSF**, Thailand Shelf-Slope Front. Red dashed lines, most probable locations of fronts. Yellow line, LME boundary.

Figure 38. Fronts of LME #38 (Indonesian Seas). Acronyms: **EBSSF**, East Borneo Shelf-Slope Front; **EFSF**, East Flores Sea fronts; **EHF**, East Halmahera Front; **EJSF**, East Java Sea fronts; **ESSSF**, East Sulawesi Shelf-Slope Front; **MaSF**, Makassar Strait Front; **MoSF**, Molucca Sea Front; **NESF**, Northeast Sulawesi Front; **SBSF**, South Banda Sea Front; **SSSSF**, Seram Sea Shelf-Slope Front. Dashed lines show most probable locations of shelf-slope fronts. Yellow line, LME boundary.

Figure 39. Fronts of LME #39 (North Australian Shelf). Acronyms: **ASF**; Arafura Sea Front; **CAF**, Cape Arnhem Front; **CYPF**, Cape York Peninsula Front; **GCF**, Gulf of Carpentaria Front; **JBGF**, Joseph Bonaparte Gulf Front. Yellow line, LME boundary.

Figure 40. Fronts of LME #40 (Northeast Australian Shelf – Great Barrier Reef). Acronyms: **NGBRF**, North Great Barrier Reef Front (most probable location); **QISF**, Queensland Inner Shelf Front; **SGBRF**, South Great Barrier Reef Front. Yellow line, LME boundary.

Figure 41. Fronts of LME #41 (East-Central Australian Shelf). Acronyms: **EACF**, East Australian Current Front. Yellow line, LME boundary.

Figure 42. Fronts of LME #42 (Southeast Australian Shelf). Acronyms: **EBSF**, East Bass Strait Front; **STF**, Subtropical Front; **TSSF**, Tasmania Shelf-Slope Front (most probable location). Yellow line, LME boundary.

Figure 43. Fronts of LME #43 (Southwest Australian Shelf). Acronyms: **LCEF**, Leeuwin Current Extension Front; **LCF**, Leeuwin Current Front; **EGABF**, East Great Australian Bight Front; **SGF**, Spencer Gulf Front; **WGABF**, West Great Australian Bight Front. Yellow line, LME boundary.

Figure 44. Fronts of LME #44 (West-Central Australian Shelf). Acronyms: **KISF**, Kalbarri Inner Shelf Front; **LCF**, Leeuwin Current Front; **NTrF**, North Tropical Front; **STrF**, South Tropical Front. Yellow line, LME boundary.

Figure 45. Fronts of LME #45 (Northwest Australian Shelf). Acronyms: **KMSF**, Kimberley Mid-Shelf Front; **NWCF**, Northwest Coastal Front. Yellow line, LME boundary.

Figure 46. Fronts of LME #46 (New Zealand Shelf). Acronyms: **ETSF**, East Tasman Front; **NCCF**, North Cape Current Front; **NSTF**, North Subtropical Front; **SCF**, Southland Current Front; **SSTF**, South Subtropical Front. Yellow line, LME boundary.

Figure 47. Fronts of LME #47 (East China Sea). Acronyms: **ECF**, East Cheju Front; **FZF**, Fujian-Zhejiang Front; **KF**, Kuroshio Front; **TCF**, Tsushima Current Front; **WCF**, West Cheju Front; **YBRF**, Yangtze Bank Ring Front. Yellow line, LME boundary.

Figure 48. Fronts of LME #48 (Yellow Sea). Acronyms: **BSF**, Bohai Sea Front; **JF**, Jiangsu Shoal Front; **KyBF**, Kyunggi (Kyonggi) Bay Front; **SPF**, Shandong Peninsula Front; **WKoBF**, West Korea Bay Front. Yellow line, LME boundary.

Figure 49. Fronts of LME #49 (Kuroshio Current). Acronyms: **OF**, Oyashio Front; **KF**, Kuroshio Front. Yellow line, LME boundary.

Figure 50. Fronts of LME #50 (Sea of Japan). Acronyms: **EKCF**, East Korea Current Front; **HSF**, Hokkaido-Sakhalin Front; **LCF**, Liman Current Front; **NKF**, North Korea Front; **SAF**, Subarctic (Subpolar) Front; **TCF**, Tsushima Current Front; **TSF**, Tsugaru Strait Front. Yellow line, LME boundary.

Figure 51. Fronts of LME #51 (Oyashio Current). Acronyms: **KOF**, Kuril-Oyashio Front. Yellow line, LME boundary.

Figure 52. Fronts of LME #52 (Sea of Okhotsk). Acronyms: **CF**, Central Front; **ESCF**, East Sakhalin Current Front; **KBF**, Kashevarov Bank Front; **MSF**, Magadan Shelf Front; **NSF**, North Shelf Front; **NWSF**, Northwest Shelf Front; **SCF**, Soya Current Front; **SGF**, Shelikhov Gulf fronts; **TBF**, TINRO Basin Front; **WKCF**, West Kamchatka Current Front. Yellow line, LME boundary.

Figure 53. Fronts of LME #53 (West Bering Sea). Acronyms: **EKCF**, East Kamchatka Current Front; **GAF**, Gulf of Anadyr Front; **KCCF**, Koryak Coast Current Front; **OSSF**, Outer Shelf-Slope Front. Yellow line, LME boundary.

Figure 54. Fronts of LME #54 (Chukchi Sea). Acronyms: **BCF**, Barrow Canyon Front; **CF**, Chukotka Front; **HSF**, Herald Shoal Front; **KSF**, Kotzebue Sound Front; **SCCF**, Siberian Coastal Current Front. Yellow line, LME boundary.

Figure 55. Fronts of LME #55 (Beaufort Sea). Acronyms: **ASSF**, Alaskan Shelf-Slope Front; **BISSF**, Banks Island Shelf-Slope Front; **MSSF**, Mackenzie Shelf-Slope Front. Yellow line, LME boundary.

Figure 56. Fronts of LME #56 (East Siberian Sea). Acronyms: **AF**, Ayon Front; **IF**, Indigirka Front; **KF**, Kolyma Front; **SCCF**, Siberian Coastal Current Front. Yellow line, LME boundary.

Figure 57. Fronts of LME #57 (Laptev Sea). Acronyms: **KREF**, Khatanga River Estuarine Front; **LREF**, Lena River Estuarine Front. Yellow line, LME boundary.

Figure 58. Fronts of LME #58 (Kara Sea). Acronyms: **OREF**, Ob’ River Estuarine Front; **WKSF**, West Kara Sea Front; **YREF**, Yenisey River Estuarine Front. Yellow line, LME boundary.

Figure 59. Fronts of LME #59 (Iceland Shelf). Acronyms: **IFF**, Iceland-Faroes Front; **ICWIF**, Irminger Current-West Iceland Front; **NIF**, North Iceland Front; **SEIF**, Southeast Iceland Front. Yellow line, LME boundary.

Figure 60. Fronts of LME #60 (Faroe Plateau). Acronyms: **FCF**, Faroe Channel Front; **FSSF**, Faroes Shelf-Slope Front. Yellow line, LME boundary.

Figure 61. Fronts of LME #61 (Antarctic). Acronyms: **ASSF**, Antarctic Shelf-Slope Front. Yellow line, LME boundary.

Figure 62. Fronts of LME #62 (Black Sea). Acronyms: **NEF**, Northeast Front; **NWF**, Northwest Front; **WSSF**, West Shelf-Slope Front.

Figure 63. Fronts of LME #63 (Hudson Bay). Acronyms: **EHBF**, East Hudson Bay Front; **NHBF**, North Hudson Bay Front; **SJBF**, South James Bay Front; **WHBF**, West Hudson Bay Front. Yellow line, LME boundary.

Figure 64. Fronts of LME #64 (Arctic Ocean). Acronyms: **AF**, Arctic Front; **LRF**, Lomonosov Ridge Front; **MARF**, Mendeleyev-Alpha Ridge Front. Yellow line, LME boundary.

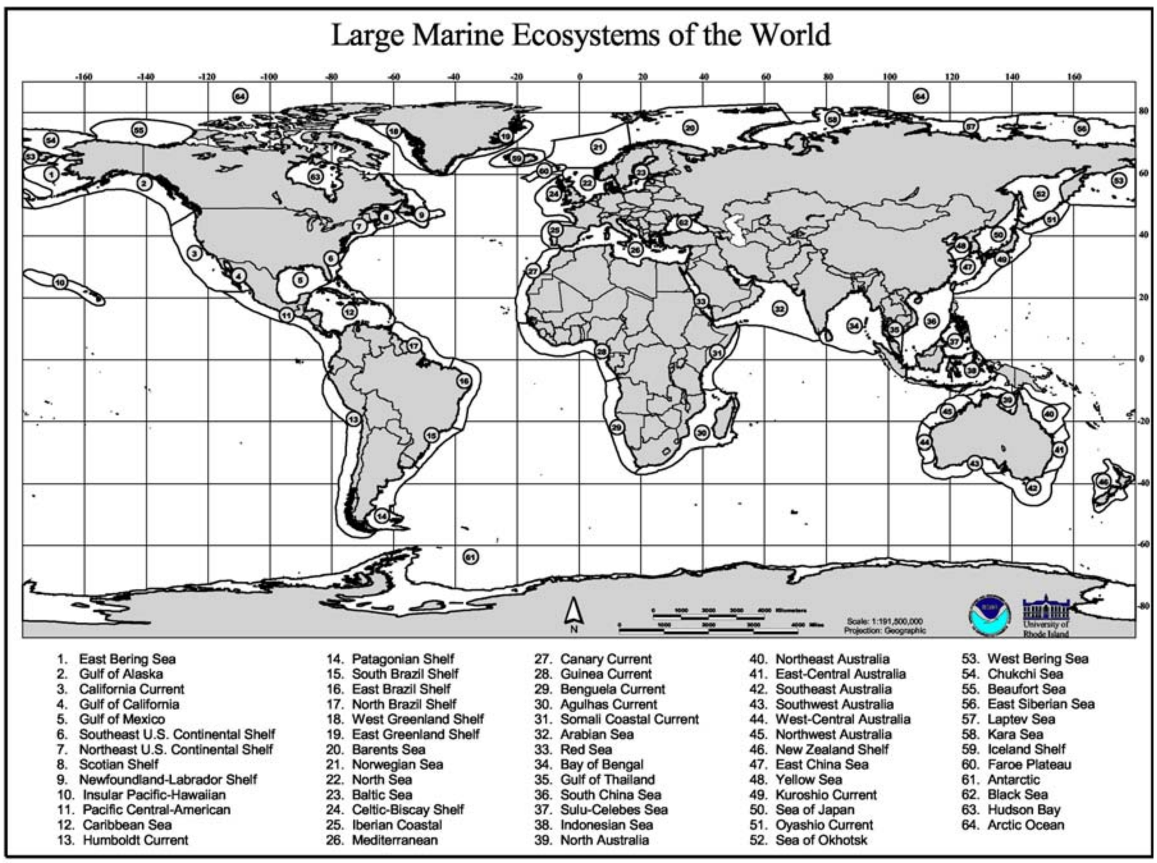

Figure 1. Large Marine Ecosystems of the World.

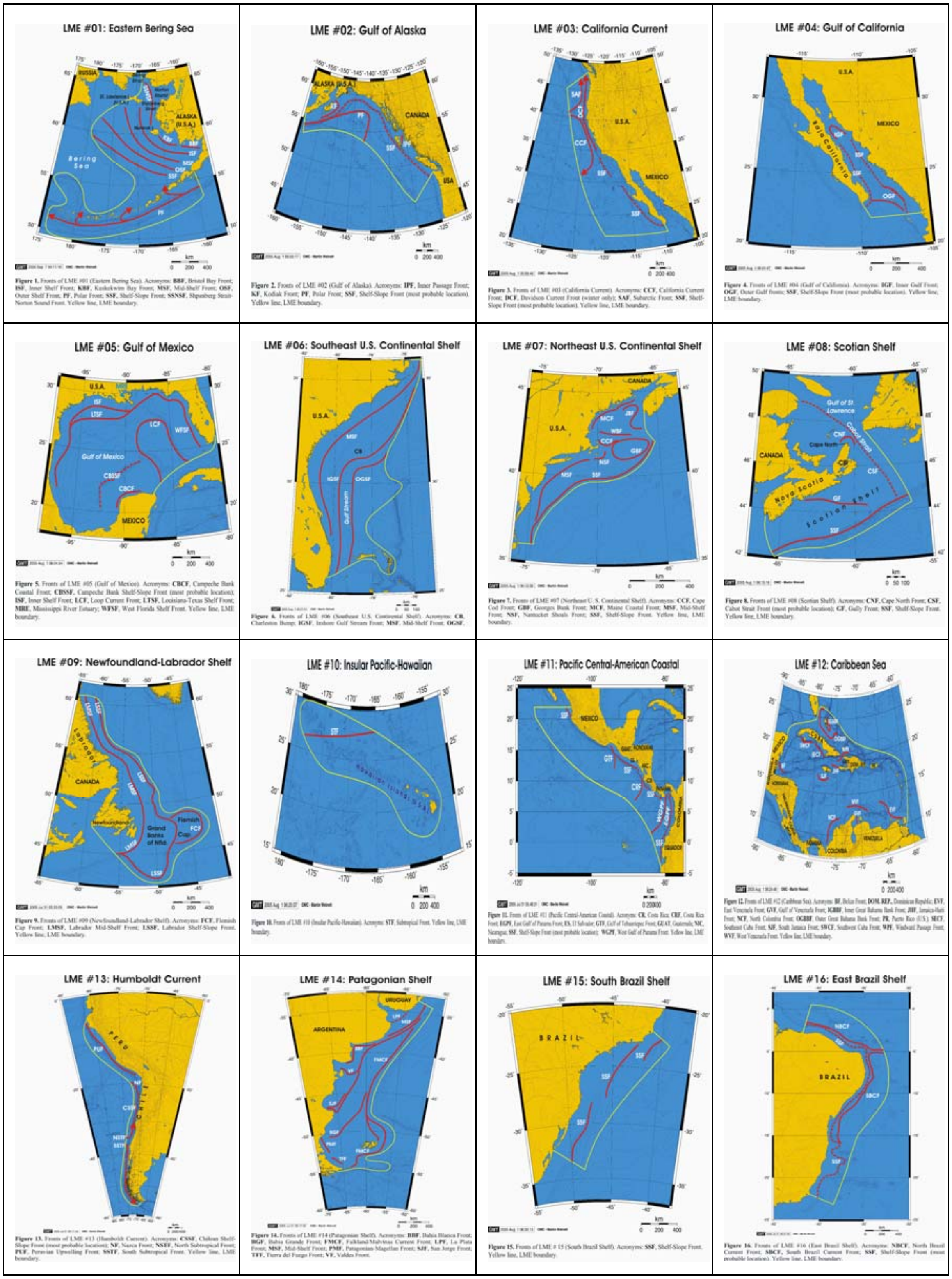

Plate 1. Frontal schematics, LME 01 through 16 (modified after Belkin, 2005).

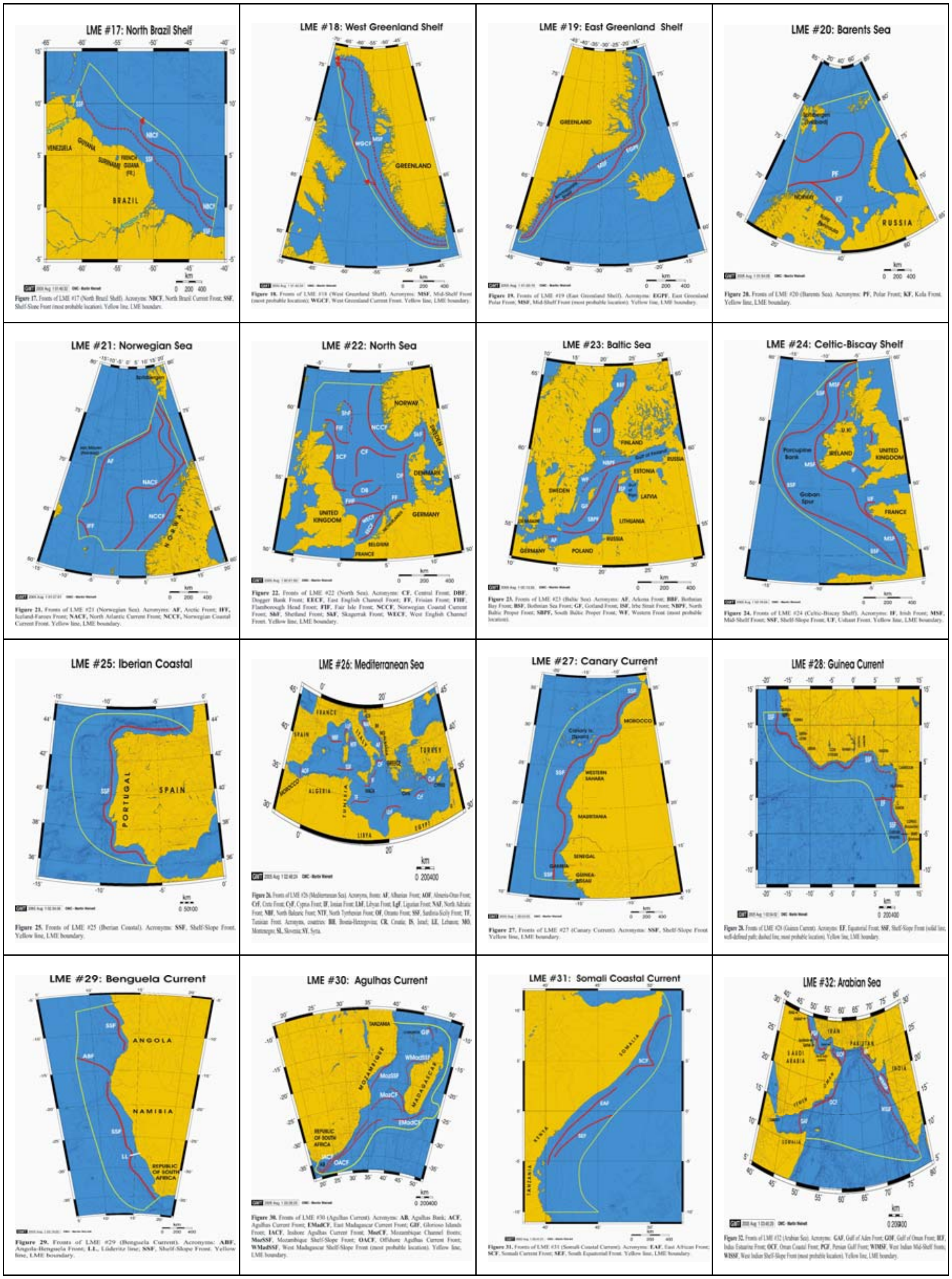

Plate 2. Frontal schematics, LME 17 through 32 (modified after Belkin, 2005).

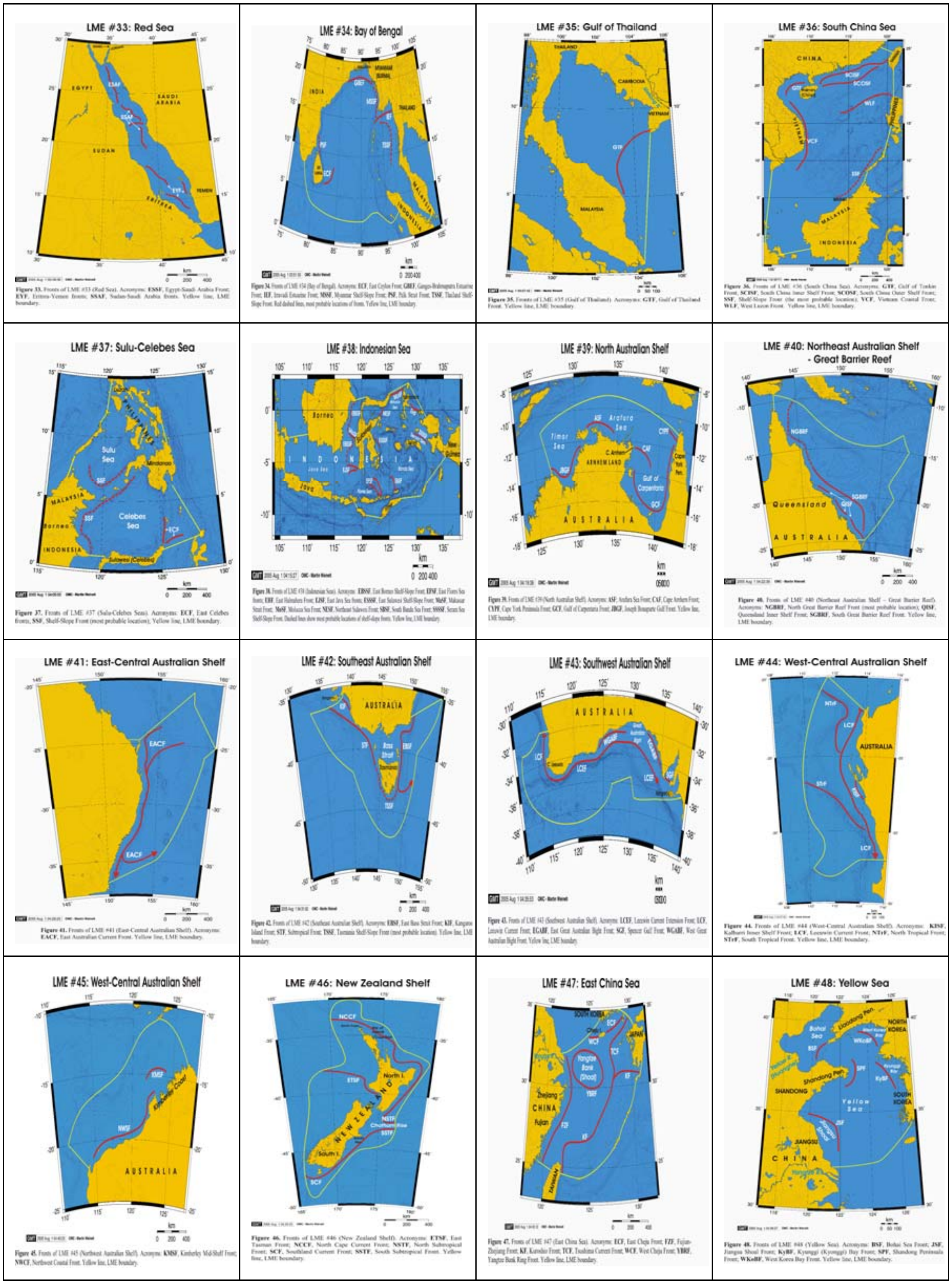

Plate 3. Frontal schematics, LME 33 through 48 (modified after Belkin, 2005).

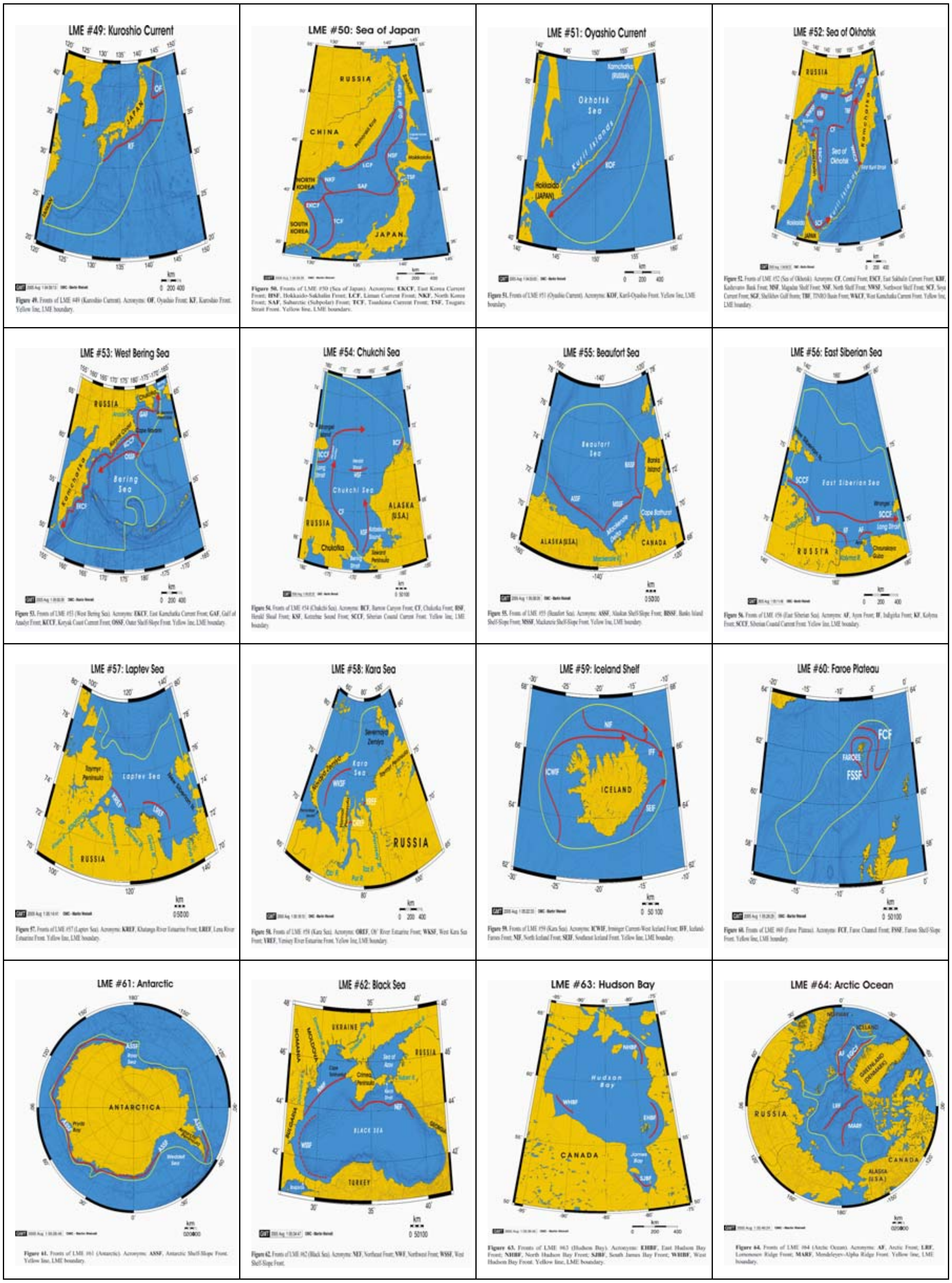

Plate 4. Frontal schematics, LME 49 through 64 (modified after Belkin, 2005).